levels relative to control. The PXR and RXRα protein levels in nuclear extracts were determined by Western blot analyses. The values are the mean ± SD for three independent experiments (*$P < 0.05$, compared with control). ***C, D,*** Schemes represent the principle of the reporter gene assay to evaluate the changes in the endogenous PXR protein level by the overexpression (***C***) or inhibition (***D***) of miR-148a. The pCYP3A4-362-7.7K plasmid contains the PXR responsive elements, ER6 (-362 to +11) and DR3 (-7836 to -7200), of the *CYP3A4* gene upstream of the *luciferase* gene. ***E, F,*** The cells were transfected with the reporter plasmid and the precursors or AsOs. After 48 h, the cells were treated with 10 μM rifampicin (square symbols) or 0.1% DMSO (circle symbols) for 24 h. The data were the firefly luciferase activities normalized with the *Renilla* luciferase activities relative to that of pGL3p plasmid without the precursors or AsOs. Each point represents the mean ± SD of three independent experiments. *$P < 0.05$, **$P < 0.01$, ***$P < 0.001$, compared with control.

FIGURE 4. **Effects of overexpression of miR-148a on the induction of endogenous CYP3A4 mRNA in LS180 cells.** ***A, B,*** The precursors for miR-148a or control (50 nM) were transfected into LS180 cells. ***A,*** After 72 h, the cells were harvested and total RNA and nuclear extracts were isolated. The mature miR-148a level was determined by real-time RT-PCR analysis. The values are the mature miR-148a levels normalized with the U6 snRNA levels relative to control. The PXR and RXRa protein levels were determined by Western blot analysis. The values are the mean ± SD of three independent experiments (**$P < 0.01$, compared with control). ***B,*** After 24, 48, 72, 96 hr, the cells were harvested and total RNA was isolated. The PXR mRNA level was determined by real-time RT-PCR analysis. The values are the PXR mRNA levels normalized with the GAPDH mRNA levels relative to control. Each point represents the mean ± SD of three independent experiments. ***C,*** Precursor-transfected LS180 cells were treated with 50 μM rifampicin or 0.1% DMSO for 24 h and then total RNA was isolated. The CYP3A4 mRNA levels were determined by real-time RT-PCR and normalized with the GAPDH mRNA level. The data are relative to that with the precursor for the control without rifampicin. Each column represents the mean ± SD of three independent experiments. ***$P < 0.001$; NS: Not significant.

FIGURE 5. **Relationship between the expression levels of miR-148a, PXR, and CYP3A4 in human liver tissue.** ***A,*** The CYP3A4 mRNA level was significantly correlated with the CYP3A4 protein levels. ***B,*** The miR-148a level was inversely correlated with the translational efficiency of PXR (PXR protein/mRNA ratio). ***C, D,*** The PXR protein level was significantly correlated with the CYP3A4 mRNA (***C***) and protein level (***D***). ***E,*** Summary of the correlation analyses (*$P < 0.05$, **$P < 0.01$, ***$P < 0.001$).

Fig. 1. Takagi *et al.*

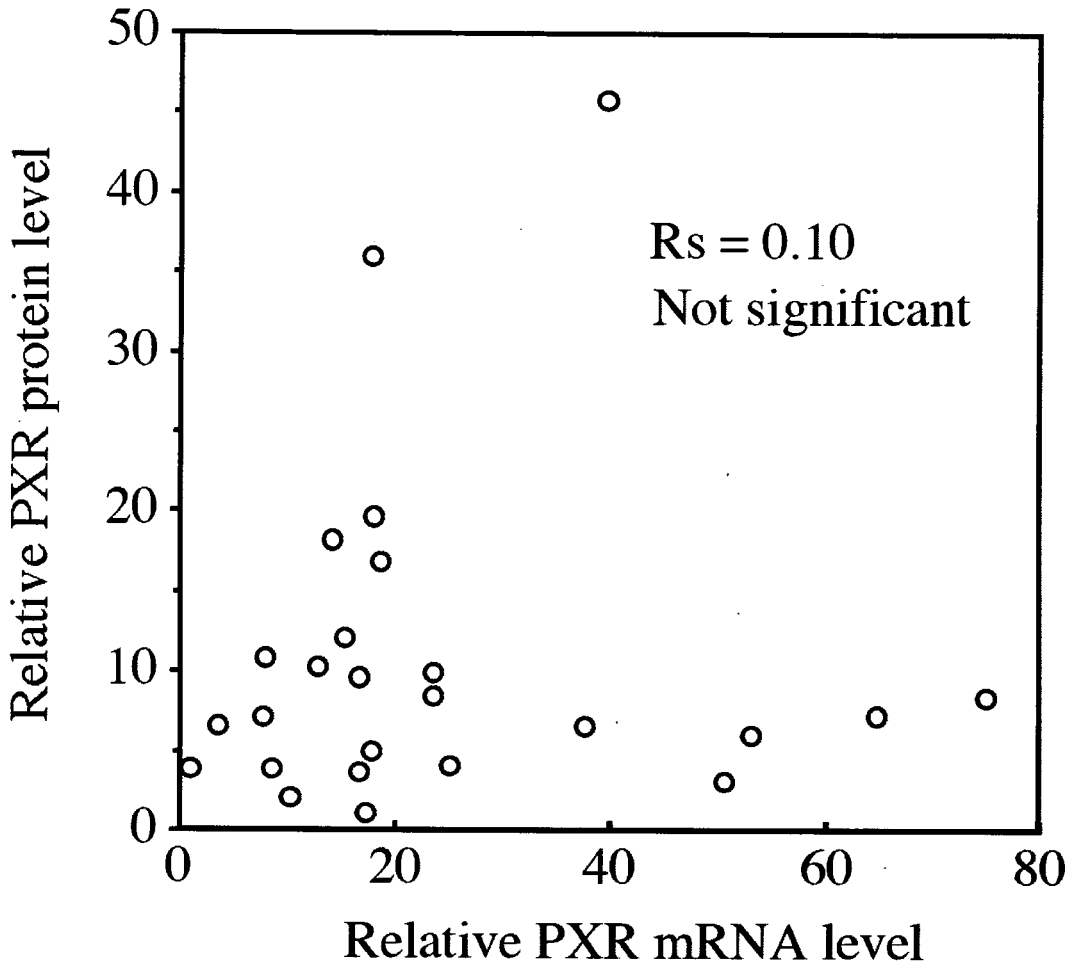

Fig. 2. Takagi et al.

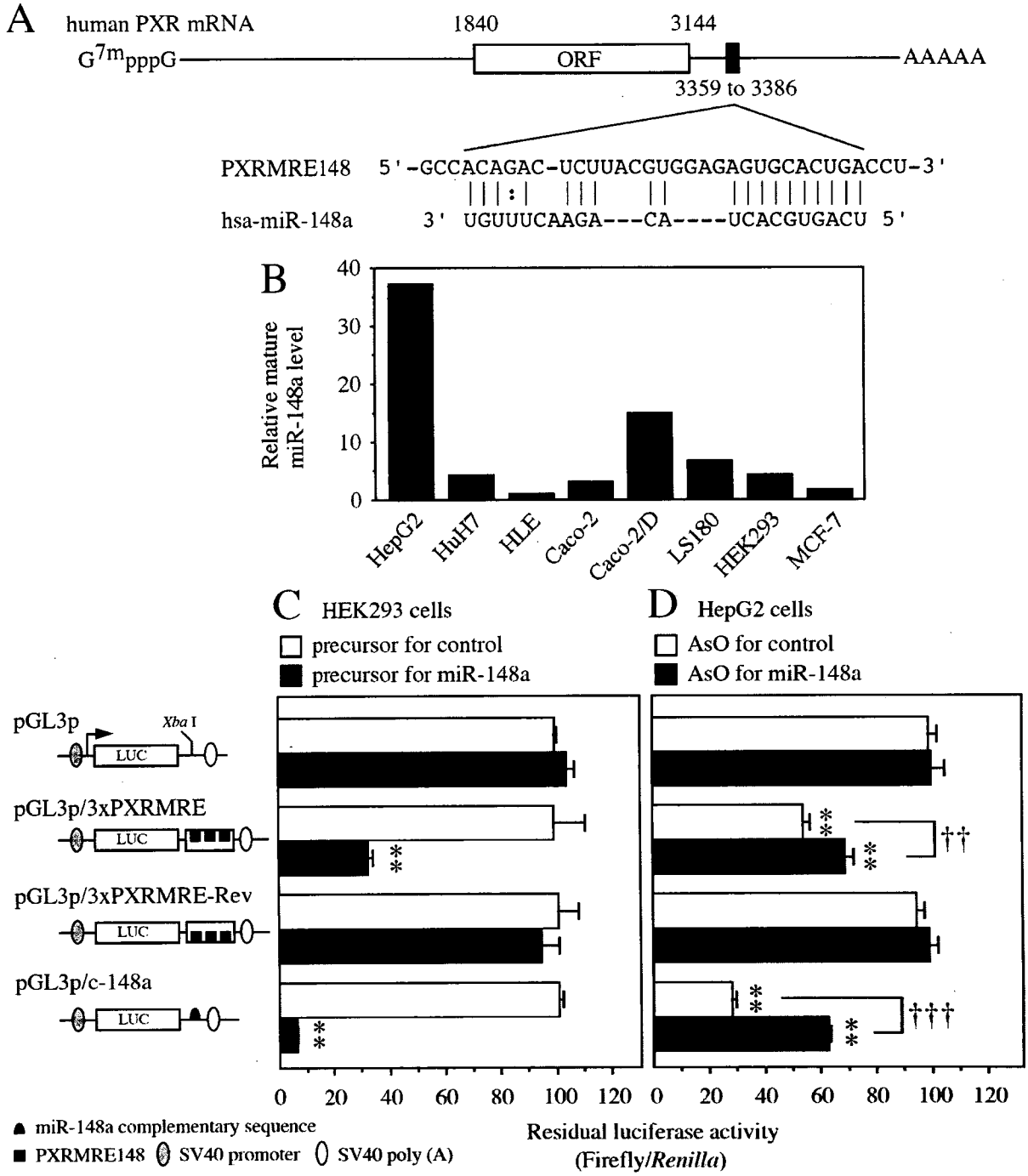

Fig. 3. Takagi et al.

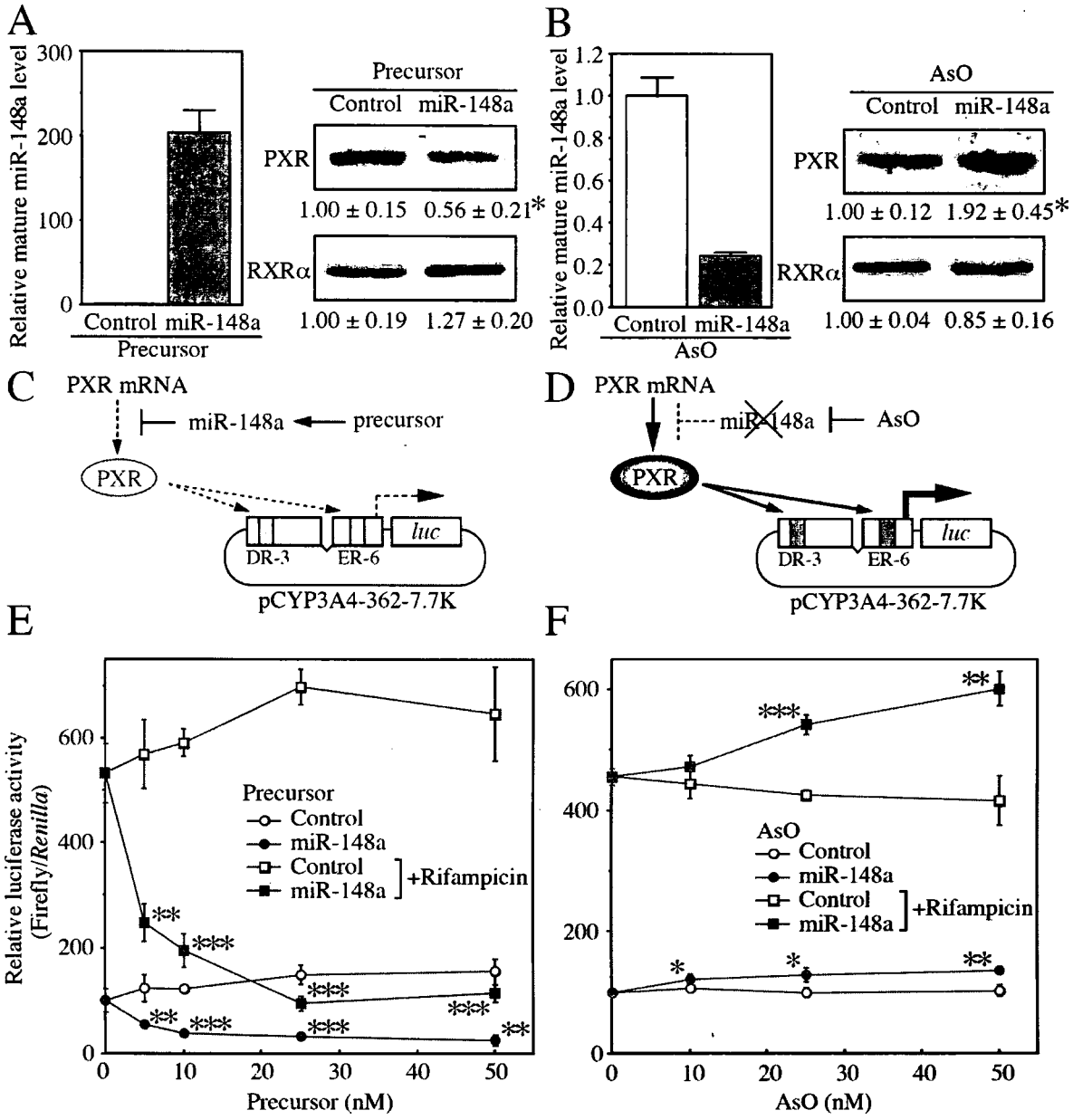

Fig. 4. Takagi et al.

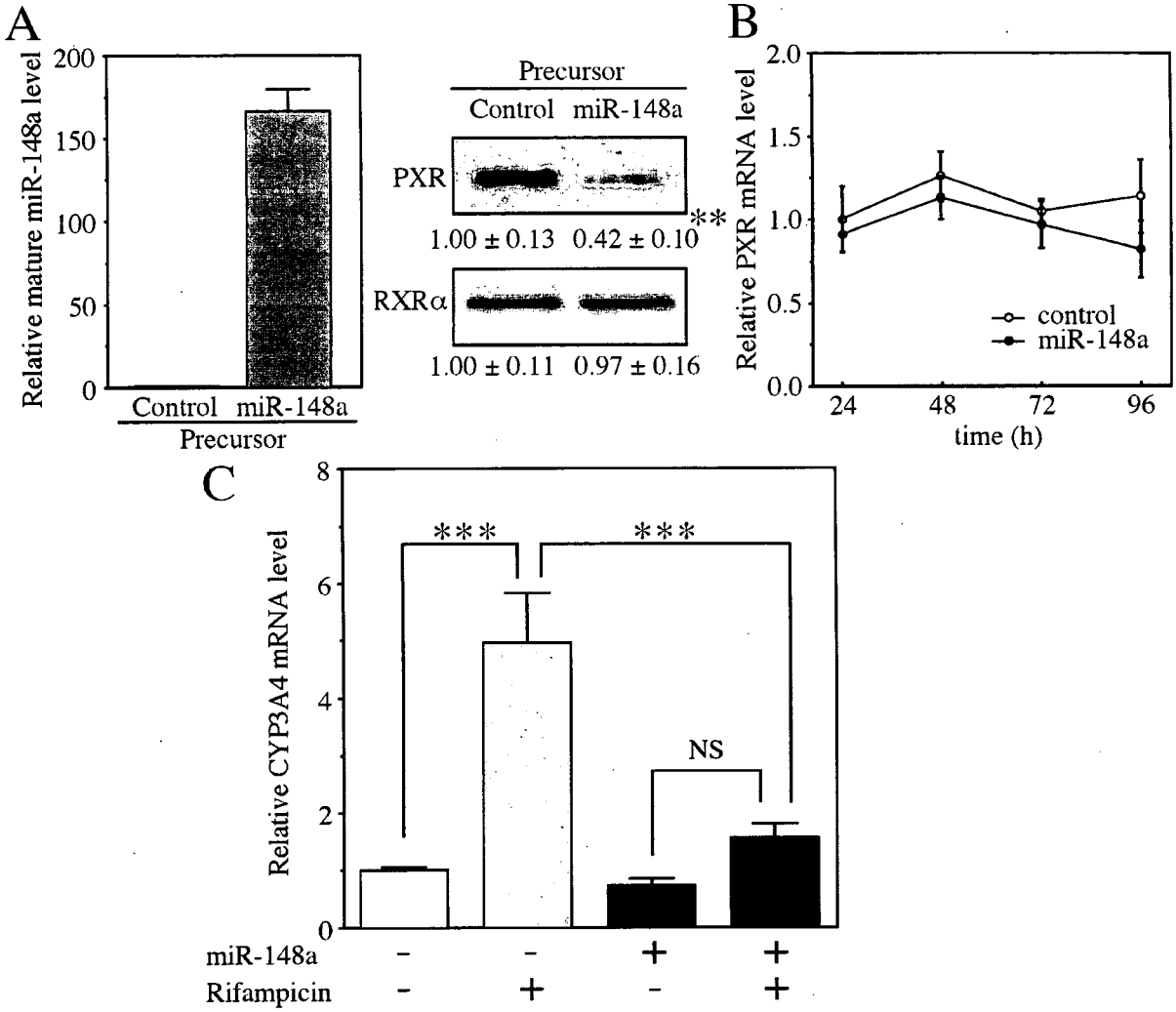

Fig. 5. Takagi et al.

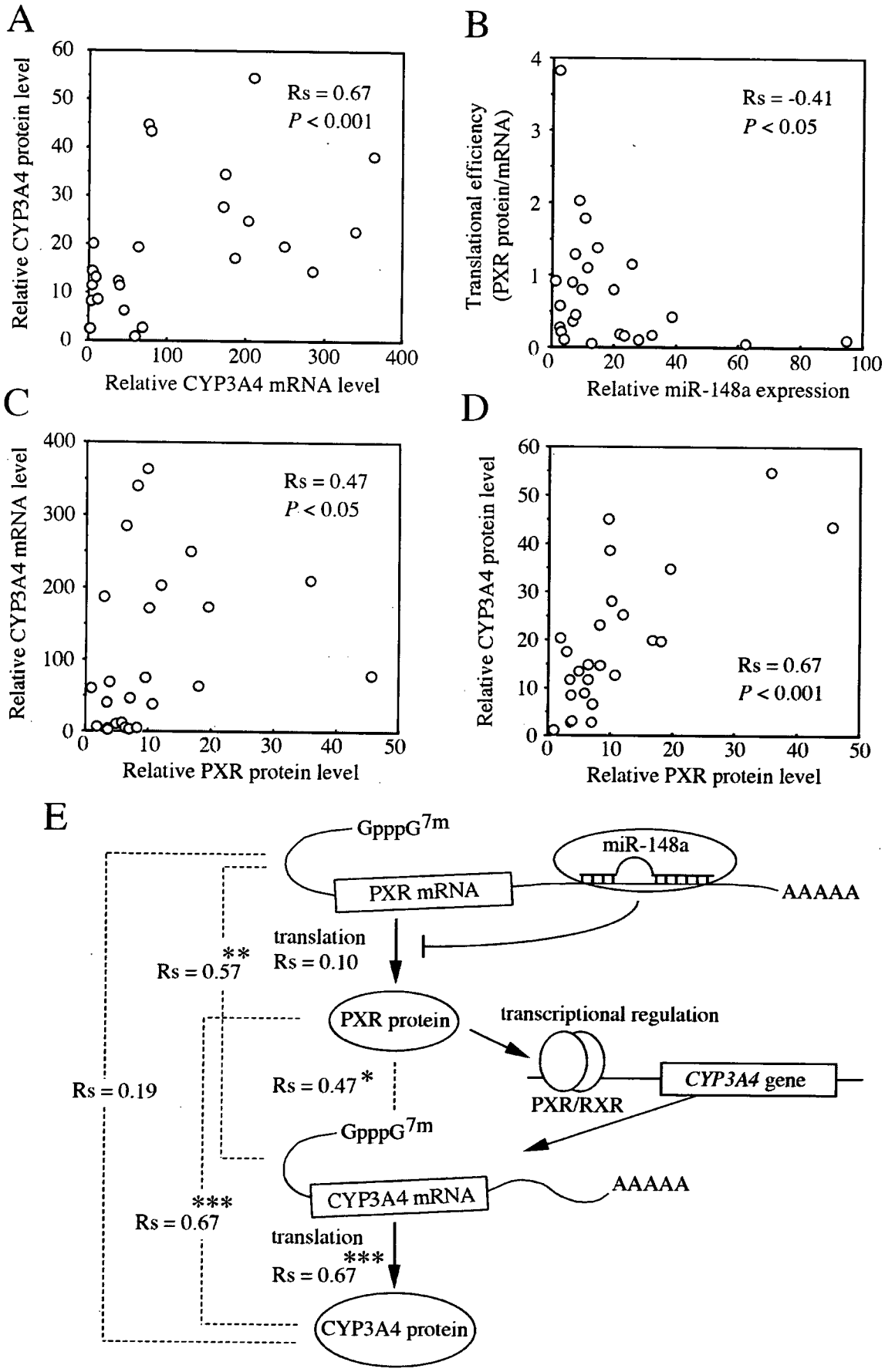

III. 研究成果の刊行に関する一覧表

別紙４

研究成果の刊行に関する一覧表

雑誌

発表者氏名	論文タイトル名	発表誌名	巻号	ページ	出版年
Sho Akai, Hiroko Hosomi, Keiichi Minami, Koichi Tsuneyama, Miki Katoh, Miki Nakajima, and Tsuyoshi Yokoi	Knock down of g-glutamylcysteine synthetase in rat causes acetaminophen-induced hepatotoxicity.	Journal of Biological Chemistry	282	23996-24003	2007
Tatsuki Fukami, Miki Nakajima, Haruko Sakai, Miki Katoh, and Tsuyoshi Yokoi	CYP2A13 metabolizes the substrates of human CYP1A2, phenacetin, and theophylline.	Drug Metabolism and Disposition	35	33-339	2007
Yusuke Hara, Miki Nakajima, Ken-ichi Miyamoto, and Tsuyoshi Yokoi	Morphine glucuronosyltransferase activity in human liver microsomes is inhibited by a variety of drugs that are co-administered with morphine.	Drug Metabolism and Pharmacokinetics	22	103-112	2007
Hirotoshi Okumura, Miki Katoh, Keiichi Minami, Miki Nakajima, and Tsuyoshi Yokoi	Change of drug excretory pathway by CCl4-induced liver dysfunction in rat.	Biochemical Phrmacology	74	488-495	2007
Hiroyuki Yamanaka, Miki Nakajima, Miki Katoh, and Tsuyoshi	Glucuronidation of thyroxine in human liver, jejunum, and kidney microsomes.	Drug Metabolism and Disposition	35	1679-1686	2007
Shinichi Takagi, Miki Nakajima, Takuya Mohri, and Tsuyoshi Yokoi	Post-transcriptional regulation of human pregnane X receptor by microRNA affects the expression of cytochrome P450 3A4.	Journal of Biolgical Chemistry		in press	
Rawiwan Maniratanachote and Tsuyoshi Yokoi	A mechanistic view of troglitazone hepatotoxicity	Hepatotoxicity: From Genomics to in vitro and in vivo. John Wiley & Sons, Ltd.		299-311	2007

THE JOURNAL OF BIOLOGICAL CHEMISTRY VOL. 282, NO. 33, pp. 23996–24003, August 17, 2007

Knock Down of γ-Glutamylcysteine Synthetase in Rat Causes Acetaminophen-induced Hepatotoxicity*

Received for publication, April 3, 2007, and in revised form, June 7, 2007 Published, JBC Papers in Press, June 15, 2007, DOI 10.1074/jbc.M702819200

Sho Akai[‡], Hiroko Hosomi[‡], Keiichi Minami[‡], Koichi Tsuneyama[§], Miki Katoh[‡], Miki Nakajima[‡], and Tsuyoshi Yokoi[‡1]

From the [‡]Division of Pharmaceutical Sciences, Graduate School of Medical Science, Kanazawa University, Kakuma-machi, Kanazawa 920-1192, Japan and [§]Department of Diagnostic Pathology, Graduate School of Medicine and Pharmaceutical Science for Research, University of Toyama, Sugitani 930-0194, Toyama, Japan

Drug-induced hepatotoxicity is mainly caused by hepatic glutathione (GSH) depletion. In general, the activity of rodent glutathione *S*-transferase is 10 to 20 times higher than that of humans, which could make the prediction of drug-induced hepatotoxicity in human more difficult. γ-Glutamylcysteine synthetase (γ-GCS) mainly regulates *de novo* synthesis of GSH in mammalian cells and plays a central role in the antioxidant capacity of cells. In this study, we constructed a GSH-depletion experimental rat model for the prediction of human hepatotoxicity. An adenovirus vector with short hairpin RNA against rat γ-GCS heavy chain subunit (GCSh) (AdGCSh-shRNA) was constructed and used to knock down the GCSh. In *in vitro* study in H4IIE cells, a rat hepatoma cell line, GCSh mRNA and protein were significantly decreased by 80% and GSH was significantly decreased by 50% 3 days after AdGCSh-shRNA infection. In the *in vivo* study in rat, the hepatic GSH level was decreased by 80% 14 days after a single dose of AdGCSh-shRNA (2×10^{11} pfu/ml/body), and this depletion continued for at least 2 weeks. Using this GSH knockdown rat model, acetaminophen-induced hepatotoxicity was shown to be significantly potentiated compared with normal rats. This is the first report of a GSH knockdown rat model, which could be useful for highly sensitive tests of acute and subacute toxicity for drug candidates in preclinical drug development.

Glutathione (5-L-glutamyl-L-cysteinylglycine, GSH)[2] is one of the most abundant tripeptides, consisting of glycine, glutamic acid, and cysteine. It serves an important function in protecting tissues against the degenerating effects of oxidative damage by scavenging free radicals from endogenous or exogenous compounds (1, 2). GSH is synthesized from its precursor amino acids in two steps of enzymatic reactions. γ-Glutamylcysteine synthetase (γ-GCS) (3) catalyzes the formation of γ-glutamylcysteine from glutamic acid and cysteine. GSH synthetase couples glycine to γ-glutamylcysteine to form GSH. γ-GCS is a rate-limiting step in GSH biosynthesis, and GSH is a feedback inhibitor of γ-GCS activity. γ-GCS is a heterodimeric enzyme composed of a catalytic subunit (heavy chain, 73 kDa) (4) and a modulatory subunit (light chain, 27.7 kDa) (5). Studies performed by purified γ-GCS suggested that the active site exists in the catalytic subunit, whereas the modulatory subunit increases the affinity of the catalytic subunit for glutamic acid and decreases the sensitivity to feedback inhibition by GSH (4). In mice, embryos homozygous for the γ-GCS heavy chain (GCSh) mutation fail to gastrulate and die (6). In contrast, homozygous knock-out mice with targeted disruption of the γ-GCS light chain are viable and fertile although the GSH level is decreased by 87% in the liver, and thus this model could be used as a GSH depletion mouse model *in vivo* (7).

Rat is the most frequently used experimental animal for pharmacological and toxicological studies in the drug development process because of their body weight and ease of sampling blood or urine. A standard technique of gene knock out in rat has not been established yet. Recently, a nuclear transfer method has been established and this method may be able to produce conditional knock out and gene replacement in the future (8), but this method is very difficult and not available for general use. Recently, recombinant adenovirus methods are being developed and used for the purpose of clinical therapy or gene delivery *in vivo* (9–11). Furthermore, a small interfering RNA strategy, which has been proven to be more specific and efficient than the full-length antisense cDNA strategy, has been established (12). In addition, an adenovirus-mediated short hairpin RNA (shRNA) knockdown approach could reduce the target gene specifically in the liver in mice, resulting in the expected phenotype (13). However, to our knowledge, there is no report that adenovirus-mediated shRNA knock down was successfully applied in rats *in vivo*. In the present study, we constructed a recombinant adenovirus (AdGCSh-shRNA) that could knock down rat GCSh mRNA efficiently *in vitro* and *in vivo*. We established the GSH-depleted rats and this rat model, when treated with acetaminophen (APAP), which is known to be biotransformed to quinoneimine (14), or some other radical species (15), demonstrated hepatotoxicity with high sensitivity compared with normal rats.

The activity of rodent glutathione *S*-transferase (GST) is about 10 to 20 times higher than that in human (16). Therefore,

* This work was supported in part by Research on Toxicogenomics, Health and Labor Science research grants from the Ministry of Health, Labor, and Welfare of Japan. The costs of publication of this article were defrayed in part by the payment of page charges. This article must therefore be hereby marked "*advertisement*" in accordance with 18 U.S.C. Section 1734 solely to indicate this fact.

[1] To whom correspondence should be addressed: Drug Metabolism and Toxicology, Division of Pharmaceutical Sciences, Graduate School of Medical Science, Kanazawa University, Kakuma-machi, Kanazawa 920-1192, Japan. Tel./Fax: 81-76-234-4407; E-mail: tyokoi@kenroku.kanazawa-u.ac.jp.

[2] The abbreviations used are: GSH, glutathione; GCS, γ-glutamylcysteine synthetase; GCSh, GCS heavy chain; shRNA, short hairpin RNA; APAP, acetaminophen; GAPDH, glyceraldehyde-3-phosphate dehydrogenase; m.o.i., multiplicity of infection; PBS, phosphate-buffered saline; CYP, cytochrome P450; pfu, plaque-forming unit; GST, glutathione S-transferase; AST, aspartate aminotransferase; ALT, alanine aminotransferase.

active metabolites produced *in vivo* in rat would be immediately detoxified by GSH conjugation, which would make the prediction of drug-induced hepatotoxicity in human more difficult. From this perspective, the AdGCSh-shRNA-mediated GSH depletion rat model could be useful for predicting the hepatotoxicity caused by unknown active metabolites of drug candidates produced by Phase I enzymes.

EXPERIMENTAL PROCEDURES

Materials—APAP and GSH were obtained from Wako Pure Chemical Industries (Osaka, Japan). β-NADPH and glutathione reductase were from Oriental Yeast (Tokyo, Japan). ISOGEN was from Nippon Gene (Tokyo, Japan). ReverTra Ace (Moloney Murine Leukemia Virus Reverse Transcriptase RNaseH Minus) was from Toyobo (Tokyo, Japan). The Adenovirus Expression Vector kit (Dual Version), random hexamer and SYBR Premix Ex Taq were from Takara (Osaka, Japan). The QuickTiter Adenovirus Titer Immunoassay kit was from Cell Biolabs (Tokyo, Japan). Lipofectamine 2000 and minimum essential α medium were from Invitrogen. The GeneSilencer shRNA Vector kit was from Gene Therapy Systems (San Diego, CA). Dulbecco's modified Eagle's medium and Ham's F12 medium were from Nissui Pharmaceutical (Tokyo, Japan). All primers and oligonucleotides for shRNA were commercially synthesized at Hokkaido System Sciences (Sapporo, Japan). Standard metabolites of APAP, such as APAP-glucuronide, APAP-sulfate, APAP-mercapturate, APAP-cysteine, and APAP-GSH, were kindly provided by McNeil Consumer Products (Washington, PA). Other chemicals were of analytical grade or the highest commercially available.

Animals—Male Fisher 344 rats (7 weeks old, 130–150 g) were obtained from SLC Japan (Hamamatsu, Japan). Animals were housed in a controlled environment (temperature 25 ± 1 °C, humidity 50 ± 10%, and 12-h light/12-h dark cycle) in the institutional animal facility with access to food and water *ad libitum*. Animals were acclimatized for a week before use for the experiments. Animal maintenance and treatment were conducted in accordance with the National Institutes of Health Guide for Animal Welfare of Japan, as approved by the Institutional Animal Care and Use Committee of Kanazawa University, Japan.

Design of Short Hairpin RNA—Rat GCSh (Gene Bank™ accession code J05181 Gene bank) knock down was achieved by RNA interference using an adenovirus vector-based shRNA approach. The sequences of shRNA-targeted GCSh cDNA were designed by B-Bridge (Mountain View, CA). The sequences of GCSh-shRNA are : top strand, 5′-gatccGTGTGAATGTCCAGAGTTAgaagcttgTAACTCTGGACATTCACACttttttggaagc-3′, and bottom strand, 5′-ggccgcttccaaaaaaGTGTGAATGTCCAGAGTTAcaagcttcTAACTCTGGACATTCACACg-3′. As a negative control, the oligonucleotide sequences of the shRNA target for luciferase from a GeneSilencer shRNA Vector kit were used.

Recombinant Adenovirus—To generate the recombinant adenovirus vector expressing GCSh-shRNA, pGSU6-GFP plasmids were recombined into the pAxcwit using the cosmide-terminal protein complex (COS-TPC) method according to the manufacturer's instruction. In brief, double strand oligo DNA for shRNA of GCSh and luciferase were inserted into the BamHI and NotI sites of the pGSU6-GFP vector. This product was digested by HincII and inserted into the SwaI site of the pAxcwit vector. This pAxcwit vector and the parental adenovirus DNA terminal protein complex were co-transfected into 293 cells by Lipofectamine 2000. The recombinant adenovirus was isolated and propagated into the 293 cells. An adenovirus containing shRNA of GCSh (AdGCSh-shRNA) and one containing shRNA of luciferase (AdLuc-shRNA) were constructed. The titer was determined by a QuickTiter Adenovirus Titer Immunoassay kit. The titers of AdGCSh- or AdLuc-shRNA were 4.95×10^{11} pfu/ml and 2.98×10^{11} pfu/ml, respectively. The viral stock solution was concentrated with the Amicon Ultra-15 filtration system (Millipore, Billerica, MA) for the *in vivo* study.

Cell Culture—The 293 cell line and rat hepatoma cell lines BRL3A and H4IIE were obtained from American Type Culture Collection (Manassas, VA). The human hepatoma cell line HLE was obtained from the Japanese Collection of Research Biosources (Tokyo, Japan). The mouse hepatoma cell line Hepa1–6 was kindly provided by Dr. S. Kaneko (Kanazawa University, Japan). The 293 cell line was maintained in Dulbecco's modified Eagle's medium containing 10% fetal bovine serum (BioWhitaker, Walkersville, MD), 3% glutamine, 16% sodium bicarbonate, and 0.1 mM nonessential amino acids (Invitrogen) in a 5% CO_2 atmosphere at 37 °C. BRL3A cells were maintained in Ham's F12, HLE and Hepa1–6 cells were maintained in Dulbecco's modified Eagle's medium, and H4IIE cells were maintained in α-minimal essential medium. All cell lines were infected by the adenovirus in medium containing 5% fetal bovine serum.

Real-time Reverse Transcription PCR Analysis—RNA from the hepatoma cells or from liver specimens was isolated using ISOGEN. Rat GCSh and glyceraldehyde-3-phosphate dehydrogenase (GAPDH) were quantified by real-time reverse transcription PCR. Primer sequences used in this study were as follows: rat GCSh, 5′-ATG CAGTATTCTGAACTACC-3′ and 5′-ACAAACTCAGATTCACCTAC-3′; mouse GCSh, 5′-TCTAACAAGAAACATCCGGCA-3′ and 5′-GGTCAGGTCGATGTCATTGTA-3′; human GCSh, 5′-ATTAGAAGAAAATCAGGCTC-3′ and 5′-GTAGCCAACTGATCATAAAG-3′; rat GAPDH, 5′-GTTACCAGGGCTGCCTTCTC-3′ and 5′-GGGTTTCCCGTTGATGACC-3′; mouse GAPDH, 5′-TCACCAGGGCTGCCATTTG-3′ and 5′-CTCACCCCATTTGATGTTAGT; human GAPDH, 5′-CCAGGGCTGCTTTTAACTC-3′ and 5′-GCTCCCCCCTGCAAATGA-3′. For the reverse transcription process, total RNA (2 μg) and 150 ng of random hexamer were mixed and incubated at 70 °C for 10 min. RNA solution was added to a reaction mixture containing 100 units of ReverTra Ace, reaction buffer, and 0.5 mM dNTPs in a final volume of 40 μl. The reaction mixture was incubated at 30 °C for 10 min, 42 °C for 1 h, and heated at 98 °C for 10 min to inactivate the enzyme. The real-time PCR was performed using the Smart Cycler (Cepheid, Sunnyvale, CA). PCR mixture contained 1 μl of template cDNA, SYBR Premix Ex Taq solution, and 10 pmol of sense and antisense primers. The PCR condition for GAPDH and GCSh were as follows. After an initial denaturation at 95 °C for 30 s, the amplification was performed by denaturation at 94 °C for 4 s, annealing and extension at 64 °C for

20 s for 45 cycles. Amplified products were monitored directly by measuring the increase of the dye intensity of the SYBR Green I (Molecular Probes, Eugene, OR) that binds to double strand DNA amplified by PCR.

Western Blot Analysis—The H4IIE cell lysates, 1.5 μg, were separated on 10% SDS-polyacrylamide gels and transferred onto polyvinylidene difluoride membrane (Immobilon-P; Millipore). The specific proteins were detected by rabbit anti-human GCSh polyclonal antibody, cross-reacting to rat GCSh (sc-22755; Santa Cruz Biotechnology, Santa Cruz, CA) at a dilution of 1:200. The protein bands were developed by biotinylated second antibody-peroxidase reaction. The quantitative analysis of protein expression was performed using ImageQuant TL Image Analysis software (Amersham Biosciences).

GSH Level—Cell lysates were mixed in 5% (w/v) metaphosphoric acid and incubated on ice for 10 min. After the addition of 0.125 M sodium phosphate buffer containing 6.3 mM EDTA, pH 7.5, the cell lysates were centrifuged at 13,000 × *g* at 4 °C for 5 min. Livers (100 mg) were homogenized with ice-cold 5% sulfosalicylic acid and centrifuged at 8,000 × *g* at 4 °C for 10 min. The GSH concentration in the supernatant was measured as described previously (17).

Adenovirus Infection and APAP Administration in Rats—Fourteen days after one intravenous injection of AdGCSh-shRNA or AdLuc-shRNA at 2×10^{11} pfu/ml/body, the rats were orally administered APAP suspended in 0.5% carboxymethylcellulose (0, 300, 1000 mg/kg body weight). Blood samples were collected at 0, 30, 60, 120, and 180 min after the APAP treatment. Twenty-four hours after the administration of APAP, serum samples were collected for assessment of transaminase levels and for APAP metabolite analysis. The liver was fixed in buffered neutral 10% formalin. The fixed samples were embedded in paraffin and sectioned at a thickness of 2 μm and stained with hematoxylin-eosin for microscopic examination. Rat liver cytosol and microsomes were prepared as described previously (18). In all experiments, the rats were not treated by fasting prior to the APAP treatment or sacrifice.

GST Activity and Cytochrome P450 (CYP) Content—The cytosolic GST activity was determined using 1-chloro-2,4-dinitrobenzene as a substrate according to the method of Habig *et al.* (19). The microsomal cytochrome P450 content was determined by the method of Omura and Sato (20).

Determination of Plasma Concentrations of APAP and Its Metabolites—The plasma concentrations of APAP and its metabolites were measured using a high performance liquid chromatography method described previously (21). In brief, plasma was mixed with an aliquot of acetonitrile containing theophylline as an internal standard. After extraction and centrifugation, the resulting supernatant was evaporated under nitrogen. The residue was diluted with distilled water as necessary before being injected into high performance liquid chromatography. APAP and its metabolites, APAP-GSH, APAP-cysteine, APAP-mercapturate, APAP-glucuronide, and APAP-sulfate, were separated in a Mightysil RP-18 column (4.6 × 150 mm; 5 μm; Kanto Chemical, Tokyo, Japan). APAP and the metabolites, eluted with 1.8% aqueous acetic acid-methanol-H_2O (66:9:100) at a flow rate of 1.0 ml/min, were monitored at 248 nm.

Statistical Analysis—Statistical analyses were performed with the GraphPad Instat version 2.0 computer program (GraphPad Software, San Diego, CA) by Student *t*-test, Dunnett's post hoc test, or Bonferroni test.

RESULTS

Changes of GCSh mRNA Expression and GSH Level in Various Hepatoma Cell Lines—To investigate the knockdown effect on the cells, various hepatoma cells were infected with AdGCSh-shRNA or AdLuc-shRNA (negative control adenovirus) at a multiplicity of infection (m.o.i.) of 20 for 3 days. Real-time reverse transcription PCR analysis and GSH assay were performed to examine the GCSh mRNA expression and GSH suppression (Fig. 1). The expression level of GCSh mRNA was significantly reduced to 20–30% in BRL3A, H4IIE, and Hepa1–6 cells. In contrast, AdGCSh-shRNA was less potent, reducing GCSh mRNA to 45% in HLE cells. The GSH level was suppressed only in H4IIE cells by 50%, despite the efficient GCSh mRNA knock down in BRL3A and Hepa1–6 cells. Based on these results, H4IIE cells were used in the next experiments.

Time-dependent Knockdown Effect of AdGCSh-shRNA in H4IIE Cells—To investigate the most efficient condition for infection, H4IIE cells were infected with AdGCSh-shRNA at m.o.i. 10 or 20 for 1, 2, 3, and 5 days. GCSh mRNA was reduced after 24 h of infection, and an 80% decrease of GCSh mRNA was achieved after 2 days of infection (Fig. 2*A*). The decrease of GCSh mRNA was accompanied by a decrease in GCSh protein (Fig. 2*B*). The GSH level was significantly reduced by 50% after 3 days of AdGCSh-shRNA m.o.i. 20 infection (Fig. 2*C*). There was no difference between 3 and 5 days of infection. These results suggested that a m.o.i. of 20 and 3 days of infection could be an appropriate condition for cytotoxicity experiments.

Effect of APAP Treatment in H4IIE Cells Infected with AdGCSh-shRNA—To investigate the effect of GSH depression on the cytotoxicity of APAP, a 3-(4,5-dimethylthiazol-2-yl)-2,5-diphenyltetrazolium bromide assay was performed. H4IIE cells were infected with AdGCSh-shRNA at m.o.i. 20 or with AdLuc-shRNA in the same conditions as a negative control. After 3 days of infection, H4IIE cells were exposed to various concentrations of APAP of 0, 0.05, 0.1, 0.25, 0.5, 1, 2.5, 5 mM. After 24 h of APAP treatment, AdGCSh-shRNA-infected cells showed no toxic effects compared with control (data not shown).

Infection of AdGCSh-shRNA to Rat—To further investigate *in vivo* in rat, a single tail vein injection to Fisher 344 rats was made to deliver AdGCSh-shRNA. The effects of GCSh knock down were examined 14 days after infection. Control animals were treated with PBS or AdLuc-shRNA. The hepatic GCSh mRNA expression was remarkably decreased dose dependently (Fig. 3*A*). At the dose of 2×10^{11} pfu/ml/body, GCSh mRNA was significantly decreased by 90%. Consistent with the decrease of GCSh mRNA, the hepatic total GSH level was also reduced to 20% at doses above 2×10^{11} pfu/ml/body (Fig. 3*B*). The hepatic GSH level in AdLuc-shRNA-infected rat was slightly increased compared with the PBS-treated rats (Fig. 3*B*).

To examine the hepatotoxic effect of the adenovirus infection, serum AST and ALT were measured 14 days after infection. As shown in Fig. 3*C*, AST was significantly elevated in the

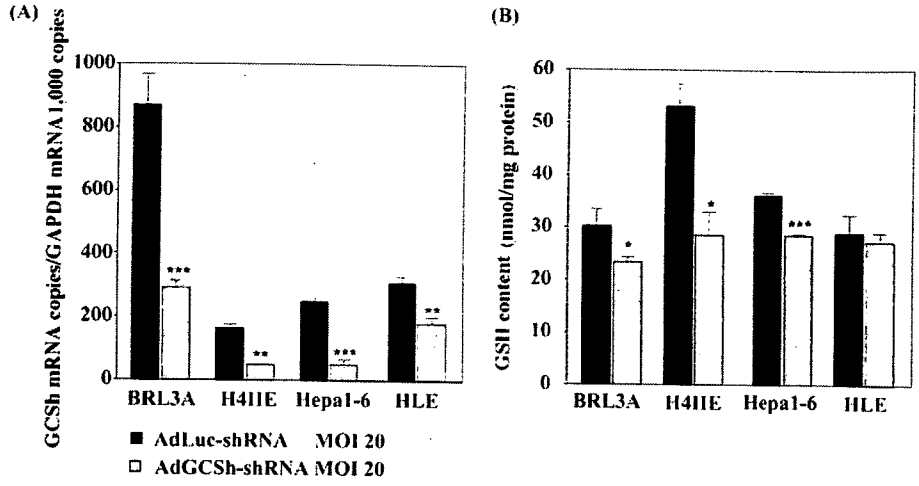

FIGURE 1. **GCSh mRNA expression and the GSH level in various hepatoma cell lines infected with AdGCSh-shRNA.** GCSh mRNA copies/GAPDH mRNA 1,000 copies (*A*) and GSH content (*B*) were determined in each cell 3 days after AdLuc-shRNA or AdGCSh-shRNA infection. Data represent the mean ± S.D. ($n = 3$). *, $p < 0.05$; **, $p < 0.01$; ***, $p < 0.001$ compared with AdLuc-shRNA infected cells.

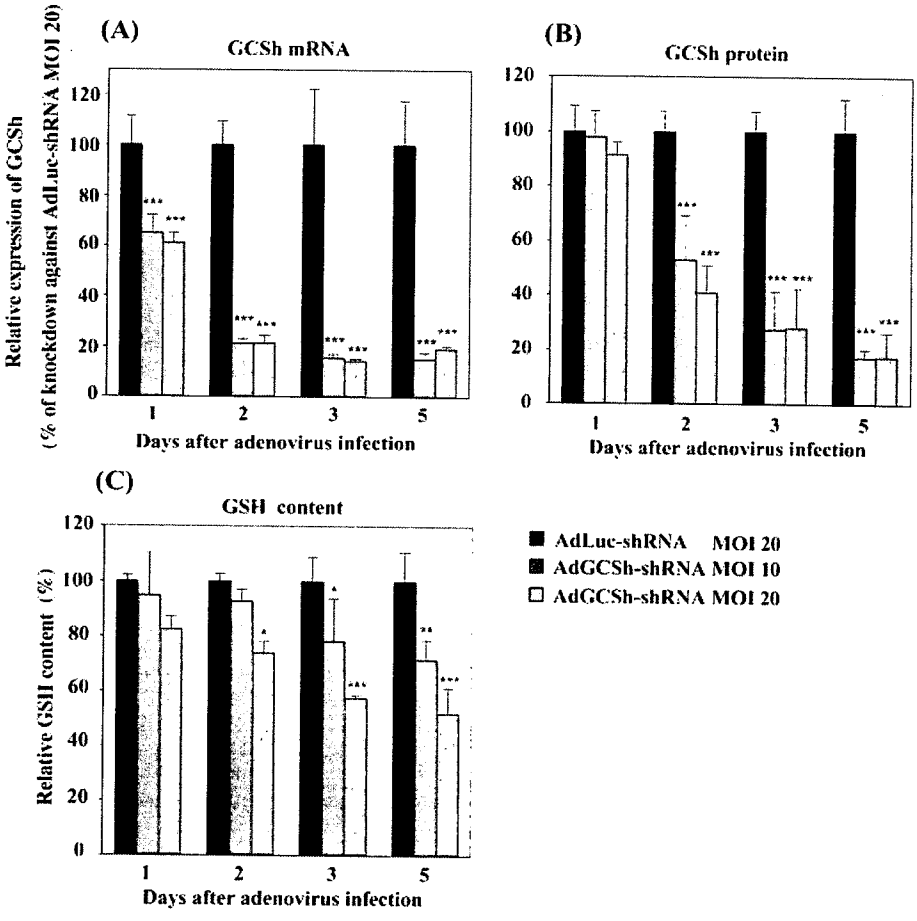

FIGURE 2. **Time-dependent knockdown effect in AdGCSh-shRNA-infected H4IIE cells.** GCSh mRNA (*A*), GCSh protein (*B*), and GSH content (*C*) were determined in H4IIE cells infected with AdLuc-shRNA or AdGCSh-shRNA. GCSh protein was quantified by immunoblotting as described under "Experimental Procedures." Data represent the mean ± S.D. ($n = 3$). *, $p < 0.05$, **, $p < 0.01$, and ***, $p < 0.001$ compared with AdLuc-shRNA-infected cells.

4.0 and 8.0 × 10^{11} pfu/ml/body infection by 1.6- and 4.1-fold, respectively, compared with the control. ALT was significantly elevated in only the 8.0 × 10^{11} pfu/ml/body infection by 2.2-fold compared with the control. The dose of 2.0 × 10^{11} pfu/ml/body did not affect the AST and ALT, and thus this condition was adopted in the next experiments. The cytochrome P450 content and GST activity slightly increased in AdGCSh-shRNA-treated rats (data not shown).

APAP-induced Hepatotoxicity in AdGCSh-shRNA-infected Rat—To determine whether APAP-induced hepatotoxicity was potentiated by the suppression of hepatic GSH, rats were tail vein-injected once with 2.0 × 10^{11} pfu/ml/body AdGCSh-shRNA or AdLuc-shRNA. After 14 days, APAP was orally administered without previous fasting. The serum AST and ALT levels are shown in Figs. 4, *A* and *B*. Twenty-four hours after APAP administration, 300 mg/kg treatment did not result in hepatotoxicity. In contrast, the AdGCSh-shRNA-infected rats treated with 1000 mg/kg APAP demonstrated a significant increase of AST (2159 ± 1156 units/liter) and ALT (924 ± 667 units/liter) compared with AdLuc-shRNA infected rats. Without fasting treatment, the AdLuc-shRNA and normal rats administered 1000 mg/kg APAP did not show hepatotoxicity. The results of the histological examination in 1000 mg/kg APAP-administered rats are shown in Fig. 4*C*. Remarkable hepatic necrosis, especially around the central vein, was observed in AdGCSh-shRNA-treated rats given 1000 mg/kg APAP, consistent with the elevation of AST and ALT. There was no histological change in the other groups.

Metabolism of APAP in Rats Infected with Adenovirus—Changes in the plasma concentration of APAP and its metabolites are shown in Fig. 5. For APAP, APAP-glucuronide, and APAP-sulfate, the maximum plasma concentration was observed 30 min or 1 h after APAP administration. The concentration of APAP-glucuronide was significantly elevated in rats infected with AdGCSh-shRNA compared with AdLuc-shRNA-infected rats (Fig. 5*B*). On the other hand, APAP-sulfate, a major detoxification product in rats generated directly from APAP, was decreased (Fig. 5*C*). For APAP-GSH, APAP-cysteine, and APAP-mercapturate, the maximum plasma concentration was observed 1 h after APAP administration in rats infected with AdGCSh-

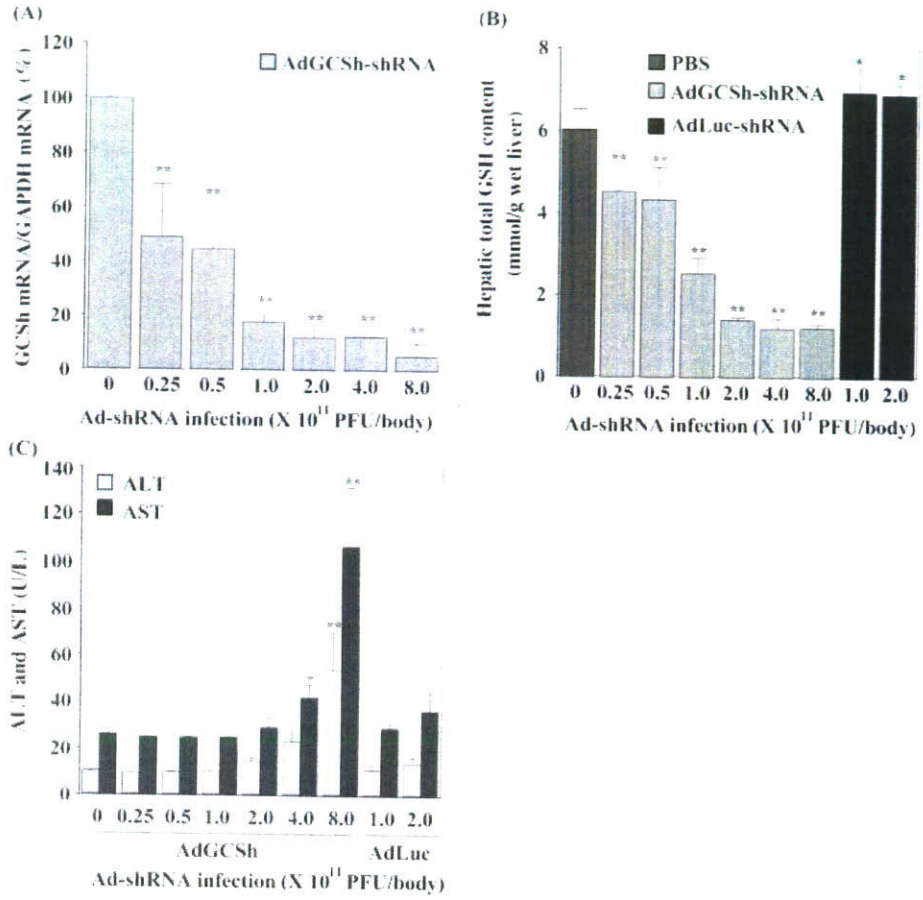

FIGURE 3. **Effects of adenovirus infection on hepatic GCSh mRNA (*A*), GSH level (*B*), ALT and AST (*C*) in rats.** All experiments were performed 14 days after AdGCSh-shRNA or AdLuc-shRNA infection. Data represent the mean ± S.D. ($n = 4$ or 5). *, $p < 0.05$ and **, $p < 0.01$ compared with PBS-treated rats or AdGCSh-shRNA-infected rats.

shRNA. As for the rats infected with AdLuc-shRNA, the concentration of APAP-GSH was gradually decreased, whereas the concentrations of APAP-cysteine and APAP-mercapturate were slightly increased.

Continuation of the Depletion of GSH Level—To examine the continuation of the hepatic GSH depletion, rats were tail vein-injected once with 2×10^{11} pfu/ml/body AdGCSh-shRNA. After 2, 3, 4, and 5 weeks, the hepatic GSH level was measured (Fig. 6). Hepatic GSH was significantly decreased by 80% at 2 to 3 weeks after infection. The hepatic GSH was reduced by 66 and 45% at 4 and 5 weeks after infection, respectively. In addition, at 7 and 10 days after infection of AdGCSh-shRNA, the hepatic GSH was decreased by 20 and 50%, respectively (data not shown). The effects of the circadian rhythm were also examined 2 weeks after infection with AdGCSh-shRNA (data not shown). The hepatic GSH level was lower than those from PBS-treated rats at all the time points examined, and no effect of the circadian rhythm on the GSH level was observed in rats infected with AdGCSh-shRNA.

DISCUSSION

In this study, a recombinant adenovirus vector expressing an shRNA-directed rat GCSh was generated (AdGCSh-shRNA). The GSH level was efficiently decreased by 50% only in H4IIE cells infected with AdGCSh-shRNA (Fig. 1). The target sequence of the rat GCSh is the same as mouse, but it differs from that of human. This would probably affect the mRNA knockdown efficiency. The lack of a decrease of GSH in BRL3A cells may be due to differences in the expression levels of coxsackie and adenovirus receptor (22).

In the cytotoxicity study, APAP treatment did not show a toxic effect in AdGCSh-shRNA-infected cells compared with AdLuc-shRNA-infected cells. APAP is mainly metabolized by UDP-glucuronosyltransferases and sulfotransferases, partly by CYP enzymes (23, 24). APAP toxicity is highly dependent upon bioactivation by CYP enzymes to the reactive intermediate N-acetyl-*p*-benzoquinoneimine (NAPQI), and a depletion of intracellular GSH would cause adduct formation targeting cellular proteins (25–28). A previous report showed that HepG2 cells which stably expressed human CYPs showed cytotoxicity by APAP, but normal HepG2 cells did not (29). H4IIE cells express no CYP enzymes (data not shown), thus APAP would not be metabolized to its toxic metabolite NAPQI and would not cause cytotoxicity.

We successfully produced a GSH-depleted rat model by means of adenovirus-mediated RNA interference technology in order to detect the drug-induced hepatotoxicity with more sensitivity than that provided by normal rats. A previous report described that infection of an adenovirus caused adenovirus-derived hepatotoxicity (30). Therefore, we validated the condition of adenovirus infection (Fig. 3). A significant increase of serum AST and ALT was observed at a high dose of AdGCSh-shRNA (8×10^{11} pfu/ml/body), suggesting adenovirus-derived hepatotoxicity (Fig. 3*C*). On the other hand, doses up to 2×10^{11} pfu/ml/body resulted in no hepatotoxicity and caused GSH depletion by 80% in rat liver. This GSH depletion level is the same as that in GCS light chain knock-out mice (7). Therefore, we determined that a single injection of AdGCSh-shRNA (2×10^{11} pfu/ml/body) was the proper condition for testing the drug-induced hepatotoxicity in this study. Furthermore, the hepatic total P450 content was slightly increased in AdGCSh-shRNA injected rats.

The maximum depletion of GSH was obtained 14 days after infection in rats in the present study, but it was obtained in 5 days in mouse (13). Because there is no previous report of adenovirus-shRNA in rats, this is the first study showing the optimum experimental condition *in vivo* in rats. In regard to the knockdown effect, the GSH level was decreased at most by 50% *in vitro* and 80% *in vivo*. This result may be due to the different

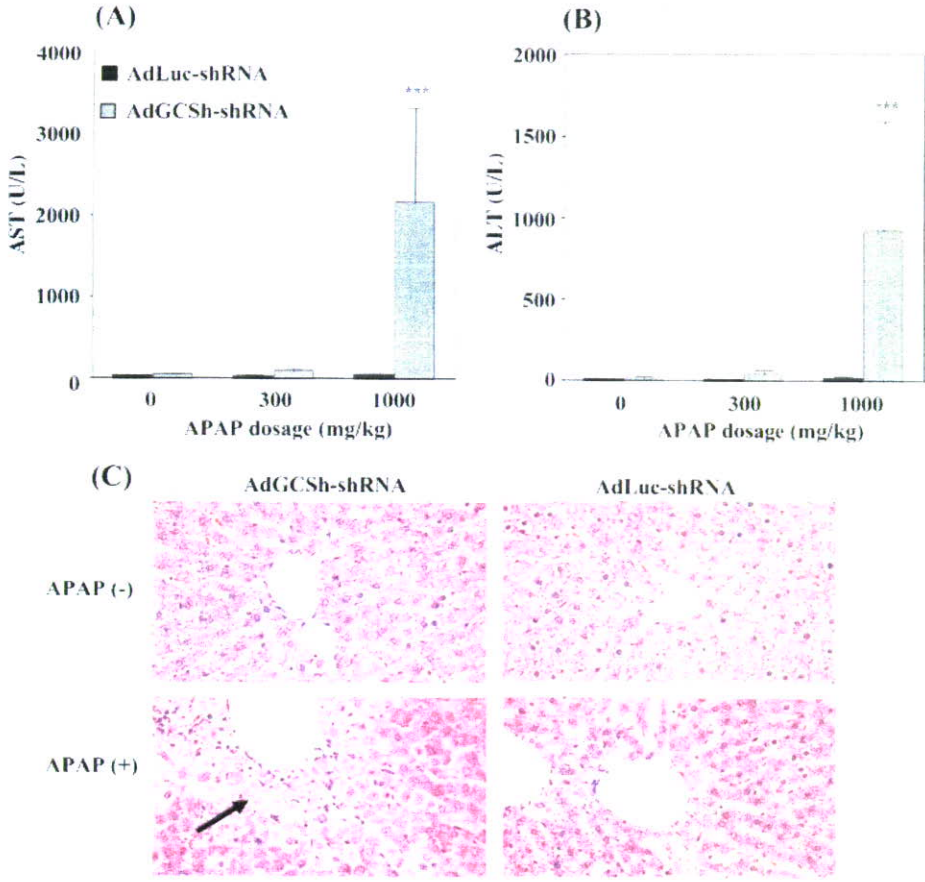

FIGURE 4. **Hepatotoxic effect of APAP in AdGCSh-shRNA-infected rats.** APAP was orally administered without previous fasting. After 24 h, serum AST (*A*) and ALT (*B*) were measured, and hematoxylin-eosin staining (*C*) was performed in sections of rat liver. Hepatic necrosis was observed only in APAP-administered rats infected with AdGCSh-shRNA. *Arrow* indicates areas of hepatic necrosis caused by 1000 mg/kg APAP treatment. Data represent the mean ± S.D. (n = 4 or 5). ***, $p < 0.001$ compared with each AdLuc-shRNA-infected group.

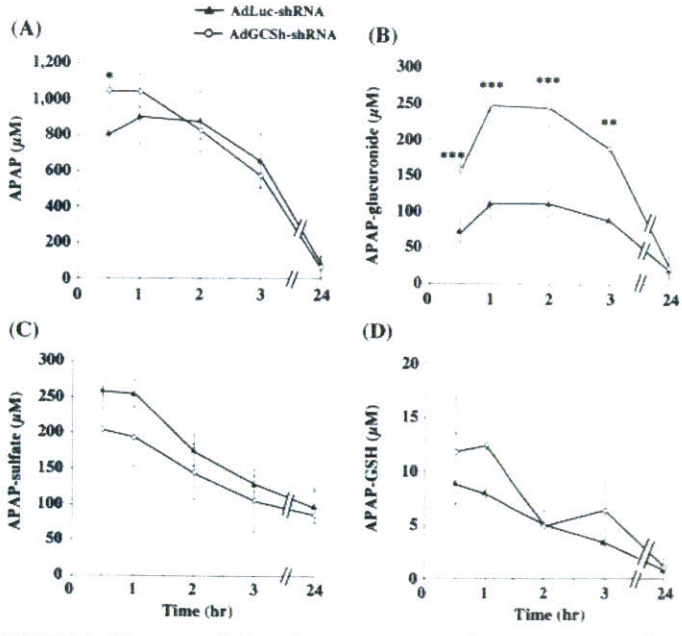

FIGURE 5. **Changes of the plasma concentrations of APAP and its metabolites in rats infected with the adenovirus.** Rats were administered APAP (1000 mg/kg, *p.o.*). Data represent the mean ± S.D. (n = 3). *, $p < 0.05$, **, $p < 0.01$, and ***, $p < 0.001$ compared with the AdLuc-shRNA-infected group.

GSH regulation mechanism, which remains to be elucidated in the future.

In previous APAP-induced hepatotoxicity studies, the rats were generally fasted for half or 1 day before drug administration (31–33). In the present study, in order to clarify the involvement of GSH depletion, the rats were not fasted before treatment. APAP-induced hepatotoxicity was observed at a single oral dose of 1000 mg/kg with fasting but was not observed without fasting (data not shown). Previous reports demonstrated that fasting caused a GSH decrease in liver (33, 34). Moreover, transcription of the CYP2E1 gene is potently activated by fasting (35). APAP is metabolized to NAPQI by CYP, mainly by CYP2E1, and thus fasting would cause an overestimation of the APAP-induced hepatotoxicity.

As an *in vivo* hepatotoxicity screening system, a single oral dose of APAP at 300 and 1,000 mg/kg to normal rats with fasting condition was reported by a Pfizer group (36), resulting in no increase of ALT and AST at 300 mg/kg after 24 h of p.o. administration, although a potent increase of ALT and AST in 1,000 mg/kg to normal rats. The same single oral administration of APAP (1,000 mg/kg) with fasting condition was also adapted by the National Toxicogenomics project in Japan as the screening system, resulting in significant increase of ALT and AST at 24 h after treatment (37). However, there is no report about the effect of fasting on APAP hepatotoxicity. In our experiments, without fasting treatment, no hepatotoxicity was observed by single oral administration of 1,000 mg/kg APAP in normal rat, as well as AdGCSh-shRNA-treated rat as shown in Fig. 4. Consequently, in our study, APAP-induced hepatotoxicity was potentiated only in rats with continuously depleted levels of GSH by AdGCSh-shRNA administration, but not by fasting. This indicated that APAP-induced hepatotoxicity would be potentiated only by the GSH depletion.

Infection of AdGCSh-shRNA caused a significant increase of APAP-glucuronide and decrease of APAP-sulfate in the plasma of the rats (Fig. 5), suggesting that GSH depletion caused the induction of UDP-glucuronosyltransferase activity. However, previous reports demonstrated that APAP-glucuronide was a substrate for multidrug resistance-associated protein 2 (MRP2) (38) and that the MRP2 expression level would change depending on the GSH concentration (39). Thus, biliary excretion of APAP-glucuronide would be decreased due to the down-regulation of MRP2 expression, and then the plasma concentration

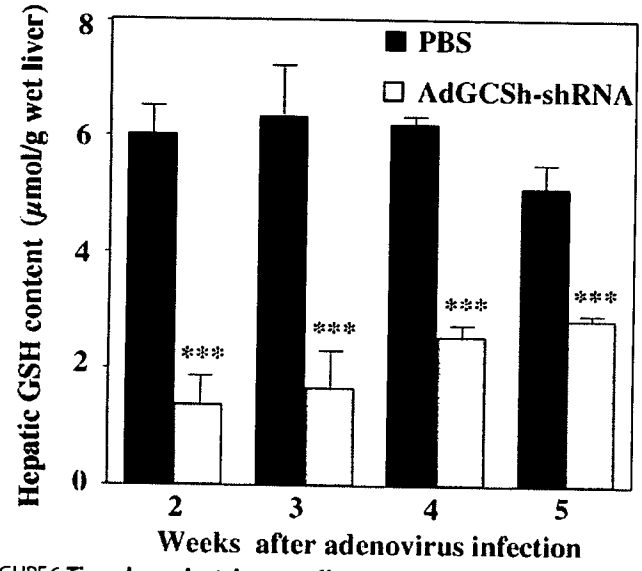

FIGURE 6. **Time-dependent changes of hepatic GSH level in rats infected with AdGCSh-shRNA.** Rat liver was excised at 2, 3, 4, and 5 weeks after infection with AdGCSh-shRNA. Data represent the mean ± S.D. (n = 3 to 5). ***, $p < 0.001$ compared with the PBS-treated group.

of APAP-glucuronide would be increased. The APAP-sulfate showed a tendency of decrease; however, the mechanism remains to be elucidated. The plasma concentrations of APAP-GSH, APAP-cysteine, and APAP-mercapturate were increased in rats infected with AdGCSh-shRNA a short time after APAP administration. The GSH depletion in liver caused by AdGCSh-shRNA slightly induced GST activity, which might be the reason for the slightly increased plasma concentrations of APAP-GSH, APAP-cysteine, and APAP-mercapturate.

Because a recombinant adenovirus is delivered predominantly to liver (40), GSH would not be reduced in other organs. However, a recent report demonstrated that a single tail vein adenovirus injection caused extra-hepatic tissue infection and expression of the target gene, especially in spleen, heart, and lung (41). Based on this report, GSH was examined in extra-hepatic tissue in the present study, but no decrease of the GSH level was observed (data not shown).

The role of GSH in the hepatotoxicity of APAP is very complex (42). Mouse lacking GST Pi was reported as showing resistance to APAP hepatotoxicity, as well as significant increased level of hepatic GSH (43). For such kind of *in vivo* hepatotoxicity studies, the present GSH knockdown system would be very useful.

Homozygous embryonic mice with targeted disruption of GCSh have been produced, but they are not viable because they fail to gastrulate (6). To generate a GSH depletion model from the perspective of gene recombination, GCS light chain knockout mice were produced that were viable and fertile and had no overt phenotype (7). Although the GSH depletion mouse model would be helpful for preclinical drug development, rats are easier to handle and scientifically reliable. Therefore, genetically modified rats are needed for further investigation. In conclusion, a hepatic GSH knockdown rat model was established for the first time in this study. To our knowledge, this is the first report demonstrating that a lethal gene was efficiently depleted by adenovirus-mediated RNA interference in rat. This rat model could be useful as a highly sensitive drug-induced hepatotoxicity test for drug candidates in preclinical drug development.

Acknowledgment—We thank Brent Bell for reviewing the manuscript.

REFERENCES

1. Reed, D. J. (1986) *Biochem. Pharmacol.* **35,** 7–13
2. Lu, S. C. (1999) *FASEB J.* **13,** 1169–1183
3. Meister, A., and Anderson, M. E. (1983) *Annu. Rev. Biochem.* **52,** 711–760
4. Huang, C. S., Chang, L. S., Anderson, M. E., and Meister, A. (1993) *J. Biol. Chem.* **268,** 19675–19680
5. Huang, C. S., Anderson, M. E., and Meister, A. (1993) *J. Biol. Chem.* **268,** 20578–20583
6. Shi, Z. Z., Osei-Frimpong, J., Kala, G., Kala, S. V., Barrios, R. J., Habib, G. M., Lukin, D. J., Danney, C. M., Matzuk, M. M., and Lieberman, M. W. (2000) *Proc. Natl. Acad. Sci. U. S. A.* **97,** 5101–5106
7. Yang, Y., Dieter, M. Z., Chen, Y., Shertzer, H. G., Nebert, D. W., and Dalton, T. P. (2002) *J. Biol. Chem.* **277,** 49446–49452
8. Zhou, Q., Renard, J. P., Le Friec, G., Brochard, V., Beaujean, N., Cherifi, Y., Fraichard, A., and Cozzi, J. (2003) *Science* **302,** 1179
9. Peng, Z. C. (2005) *Hum. Gene Ther.* **16,** 1016–1027
10. Chu, R. L., Post, D. E., Khuri, F. R., and Van Meir, E. G. (2004) *Clin. Cancer Res.* **10,** 5299–5312
11. Kruyt, F. A., and Curiel, D. T. (2002) *Hum. Gene Ther.* **13,** 485–495
12. Meister, G., and Tuschl, T. (2004) *Nature* **431,** 343–349
13. Xu, H., Wilcox, D., Nguyen, P., Voorbach, M., Suhar, T., Morgan, S. J., An, W. F., Ge, L., Green, J., and Wu, Z. (2006) *Biochem. Biophys. Res. Commun.* **349,** 439–448
14. Dahlin, D. C., Miwa, G. T., Lu, A. Y., and Nelson, S. D. (1984) *Proc. Natl. Acad. Sci. U. S. A.* **81,** 327–331
15. Moldeus, P., Andersson, B., Rahimtula, A., and Berggren, M. (1982) *Biochem. Pharmacol.* **31,** 1363–1368
16. Grover, P. L., and Sims, P. (1964) *Biochem. J.* **90,** 603–606
17. Tietze, F. (1969) *Anal. Biochem.* **27,** 502–522
18. Guengerich, F. P., Shimada, T., Yun, C. H., Yamazaki, H., Raney, K. D., Their, R., Coles, B., and Harris, T. M. (1994) *Environ. Health Perspect.* **102,** (Suppl.) 49–53
19. Habig, W. H., Pabst, M. J., and Jakoby, W. B. (1974) *J. Biol. Chem.* **249,** 7130–7139
20. Omura, T., and Sato, R. (1964) *J. Biol. Chem.* **239,** 2370–2378
21. Kim, Y. C., and Lee, S. J. (1998) *Toxicology* **128,** 53–61
22. Huang, K. C., Altinoz, M., Wosik, K., Larochelle, N., Koty, Z., Zhu, L., Holland, P. C., and Nalbantoglu, J. (2005) *Int. J. Cancer* **113,** 738–745
23. Howie, D., Adriaenssens, P., and Prescott, L. F. (1977) *J. Pharm. Pharmacol.* **29,** 235–237
24. Tone, Y., Kawamata, K., Murakami, T., Higashi, Y., and Yata, N. (1990) *J. Pharmacobio-dyn* **13,** 327–335
25. Miner, D. J., and Kissinger, P. T. (1979) *Biochem. Pharmacol.* **28,** 3285–3290
26. Hinson, J. A., Pohl, L. R., Monks, T. J., and Gillette, J. R. (1981) *Life Sci.* **29,** 107–116
27. Albano, E., Rundgren, M., Harvison, P. J., Nelson, S. D., and Moldeus, P. (1985) *Mol. Pharmacol.* **28,** 306–311
28. van de Straat, R., Vromans, R. M., Bosman, P., de Vries, J., and Vermeulen, N. P. (1988) *Chem. Biol. Interact.* **64,** 267–280
29. Yoshitomi, S., Ikemoto, K., Takahashi, J., Miki, H., Namba, M., and Asahi, S. (2001) *Toxicol. In Vitro* **3,** 245–256
30. Callahan, S. M., Boquet, M. P., Ming, X., Brunner, L. J., and Croyle, M. A. (2006) *J. Gene Med.* **8,** 566–576
31. Merrick, B. A., Bruno, M. E., Madenspacher, J. H., Wetmore, B. A., Foley, J., Pieper, R., Zhao, M., Makusky, A. J., McGrath, A. M., and Zhou, J. X. (2006) *J. Pharmacol. Exp. Ther.* **318,** 792–802
32. Kim, Y. W., Ki, S. H., Lee, J. R., Lee, S. J., Kim, C. W., Kim, S. C., and Kim, S. G. (2006) *Chem. Biol. Interact.* **161,** 125–138
33. Pessayre, D., Wandscheer, J. C., Cobert, B., Level, R., Degott, C., Batt, A. M., Martin, N., and Benhamou, J. P. (1980) *Biochem. Pharmacol.* **29,**

2219–2223
34. Jaeschke, H., and Wendel, A. (1985) *Biochem. Pharmacol.* **34,** 1029–1033
35. Johansson, I., Lindros, K. O., Eriksson, H., and Ingelman-Sundberg, M. (1990) *Biochem. Biophys. Res. Commun.* **173,** 331–338
36. Kikkawa, R., Fujikawa, M., Yamamoto, T., Hamada,Y., Yamada, H., and Horii, I. (2006) *J. Toxicol. Sci.* **31,** 23–34
37. Morishita, K., Mizukawa, Y., Kasahara, T., Okuyama, M., Takashima, K., Toritsuka, N., Miyagishima, T., Nagao, T., and Urushidani, T. (2006) *J. Toxicol. Sci.* **31,** 491–507
38. Xiong, H., Turner, K. C., Ward, E. S., Jansen, P. L., and Brouwer, K. L. (2000) *J. Pharmacol. Exp. Ther.* **295,** 512–518
39. Sekine, S., Ito, K., and Horie, T. (2006) *Free Radic. Biol.* **40,** 2166–2174
40. Hayder, H., Blanden, R. V., Korner, H., Riminton, D. S., Sedgwick, J. D., and Mullbacher, A. (1999) *J. Immunol.* **163,** 1516–1520
41. Crettaz, J., Berraondo, P., Mauleon, I., Ochoa, L., Shankar, V., Barajas, M., van Rooijen, N., Kochanek, S., Qian, C., and Prieto, J. (2006) *Hepatology* **44,** 623–632
42. Farkas, D., and Tannenbaum, S. R. (2005) *Curr. Drug Metab.* **6,** 111–125
43. Henderson, C. J., Wolf, C. R., Kitteringham, N., Powell, H., and Park, B. K. (2000) *Proc. Natl. Acad. Sci. U. S. A.* **97,** 12741–12745

0090-9556/07/3503-335–339$20.00
DRUG METABOLISM AND DISPOSITION

DMD 35:335–339, 2007

Vol. 35, No. 3
11064/3183027
Printed in U.S.A.

Short Communication

CYP2A13 Metabolizes the Substrates of Human CYP1A2, Phenacetin, and Theophylline

Received October 24, 2006; accepted December 15, 2006

ABSTRACT:

Human cytochrome CYP2A13 shows overlapping substrate specificity with CYP2A6, catalyzing the metabolism of coumarin, nicotine, cotinine, and 4-(methylnitrosamino)-1-(3-pyridyl)-1-butanone. Recently, it was found that CYP2A13 could catalyze the metabolic activations of 4-aminobiphenyl and aflatoxin B_1, which are known to be catalyzed by human CYP1A2. In the present study, we investigated the substrate specificity of CYP2A13. It was shown that CYP2A13 could catalyze ethoxyresorufin *O*-deethylation, methoxyresorufin *O*-demethylation, and phenacetin *O*-deethylation, which are used as marker activities for human CYP1A2. Although the intrinsic clearances (V_{max}/K_m) of the two former reactions by CYP2A13 were much lower than that of CYP1A2, the value of the last reaction by CYP2A13 was 2-fold higher than that of CYP1A2. Of particular interest was that CYP2A13 has higher affinity toward phenacetin than CYP1A2. In contrast, CYP2A6 hardly catalyzed these reactions, although the amino acid identity with CYP2A13 is as high as 93.5%. Furthermore, we found that CYP2A13 can catalyze theophylline 8-hydroxylation and 3-demethylation, which are known to be mainly catalyzed by human CYP1A2, although the intrinsic clearances were approximately one-tenth that of CYP1A2. CYP2A13 would not contribute to the systemic clearance of these drugs because CYP2A13 is hardly expressed in human liver. However, it may play a role in metabolism in local tissues such as lung or trachea. In conclusion, the results of the present study could extend our understanding of the substrate specificity of CYP2A13.

The human *CYP2A* gene subfamily comprises two functional genes, *CYP2A6* (Yamano et al., 1990) and *CYP2A13* (Su et al., 2000), and a nonfunctional gene, *CYP2A7* (Yamano et al., 1990). CYP2A6 is mainly expressed in the liver, whereas CYP2A13 is predominantly expressed in the respiratory tract, with the highest level in the nasal mucosa, followed by the lung and trachea (Koskela et al., 1999; Gu et al., 2000; Su et al., 2000). Both CYP2A6 and CYP2A13 are composed of 494 amino acids with a high degree of identity (93.5%). CYP2A6 is involved in the metabolism of coumarin and nicotine and the metabolic activation of tobacco-specific nitrosamines such as 4-(methylnitrosamino)-1-(3-pyridyl)-1-butanone (Yamano et al., 1990; Tiano et al., 1993; Nakajima et al., 1996). CYP2A13 is also active toward these CYP2A6 substrates (Su et al., 2000; von Weymarn and Murphy, 2003; Bao et al., 2005). Although CYP2A13 is less active for coumarin 7-hydroxylation than CYP2A6, it is much more active for nicotine, cotinine, and especially 4-(methylnitrosamino)-1-(3-pyridyl)-1-butanone metabolisms (Su et al., 2000; He et al., 2004; Bao et al., 2005). Thus, although there are distinct overlaps in the substrate specificities of CYP2A6 and CYP2A13, the catalytic efficiencies differ between the two isoforms.

Recently, we found that CYP2A13 could catalyze the metabolic activation of 4-aminobiphenyl (Nakajima et al., 2006). Furthermore, it has been reported that CYP2A13 is active for the metabolism of aflatoxin B_1 (He et al., 2006). In contrast, CYP2A6 is not active for these substrates. These activities had been known to be catalyzed by CYP1A2 (Gallagher et al., 1996; Hammons et al., 1997). In the present study, we investigated whether CYP2A13 has the ability to metabolize the compounds that are representative substrates of CYP1A2.

T.F. was supported as a Research Fellow of the Japan Society for the Promotion of Science.

Article, publication date, and citation information can be found at http://dmd.aspetjournals.org.

doi:10.1124/dmd.106.011064.

Materials and Methods

Chemicals. Coumarin, 7-hydroxycoumarin, acetaminophen, theophylline, 1-methylxanthine (1-MX), 3-methylxanthine (3-MX), 1,3-dimethyluric acid (1,3-DMU), and theobromine were obtained from Wako Pure Chemicals (Osaka, Japan). Phenacetin, ethoxyresorufin, methoxyresorufin, and resorufin were from Sigma-Aldrich (St. Louis, MO). All the other chemicals and solvents were of analytical grade or the highest grade commercially available.

Enzyme Preparations. *Escherichia coli* membranes expressing recombinant human CYP1A1/NPR (Yamazaki et al., 2002), CYP1A2/NPR (Yamazaki et al., 2002), CYP2A6/NPR (Fukami et al., 2004), and CYP2A13/NPR (Yamanaka et al., 2005) were previously prepared in our laboratory. The cytochrome P450 (P450) content and protein concentration were determined according to a method described previously (Omura and Sato, 1964; Bradford, 1976). NADPH-cytochrome *c* reductase activity was determined as described previously (Williams and Kamin, 1962; Yasukochi and Masters, 1976) using $\Delta_{\varepsilon 550}$ = 21.1 mM/cm, and the content was calculated using the specific activity of 3.0 μmol reduced cytochrome *c*/min/nmol NPR based on purified rabbit NPR preparations (Parikh et al., 1997).

Enzyme Assays. Coumarin 7-hydroxylation was determined as described previously (Ohyama et al., 2000). The substrate concentration was 0.1 to 5 μM. Ethoxyresorufin *O*-deethylation and methoxyresorufin *O*-demethylation were determined as described previously (Nakajima et al., 1998). The concentrations of ethoxyresorufin and methoxyresorufin were 0.1 to 2.5 μM for CYP1A1 and CYP1A2 or 0.5 to 7.5 μM for CYP2A6 and CYP2A13.

ABBREVIATIONS: 1-MX, 1-methylxantine; 3-MX, 3-methylxantine; 1,3-DMU, 1,3-dimethyluric acid; P450, cytochrome P450; HPLC, high-performance liquid chromatography.

Phenacetin *O*-deethylation was determined as follows: a typical incubation mixture (final volume of 0.2 ml) contained the *E. coli* membrane preparation (5 pmol of P450), 100 mM potassium phosphate buffer (pH 7.4), an NADPH-generating system (0.5 mM $NADP^+$, 5 mM glucose 6-phosphate, 5 mM $MgCl_2$, and 1 U/ml glucose-6-phosphate dehydrogenase), and 10 to 250 μM phenacetin. The reaction was initiated by the addition of the NADPH-generating system after 2-min preincubation at 37°C. After the 20-min incubation at 37°C, the reaction was terminated by the addition of 10 μl of 60% perchloric acid. After the removal of protein by centrifugation at 10,000 rpm for 5 min, a 20-μl portion of the supernatant was subjected to high-performance liquid chromatography (HPLC). HPLC analyses were performed using an L-7100 pump (Hitachi, Tokyo, Japan), L-7200 autosampler (Hitachi), and a D-2500 integrator (Hitachi) equipped with a Mightysil RP-18 C18 GP (4.6 × 150 mm, 5 μm) column (Kanto Chemical, Tokyo, Japan). The eluent was monitored at 245 nm. The mobile phase was 8% acetonitrile containing 50 mM potassium phosphate (pH 4.2). The flow rate was 1.0 ml/min. The column temperature was 35°C. The quantification of acetaminophen was performed by comparing the HPLC peak height with that of an authentic standard.

Theophylline demethylation and hydroxylation were determined as follows: a typical incubation mixture (final volume of 0.5 ml) contained an *E. coli* membrane preparation (5 pmol of P450), 100 mM potassium phosphate buffer (pH 7.4), an NADPH-generating system, and 0.1 to 125 mM theophylline. The reaction was initiated by the addition of the NADPH-generating system after 2-min preincubation at 37°C. After the 30-min incubation at 37°C, the reaction was terminated by the addition of 25 μl of 1 M hydroxychloride. Theobromine (250 pmol) was added as an internal standard. The reaction mixture was extracted with 5 ml of dichloromethane/isopropyl alcohol (75:25 v/v) and then centrifuged at 2000 rpm for 10 min to separate the aqueous and organic fractions. The organic fraction was evaporated under a gentle stream of nitrogen at 40°C. The residue was redissolved in 100 μl of mobile phase, and then the 50-μl portion of the sample was subjected to HPLC. The HPLC apparatus was the same as described above except for a Mightysil RP-18 C18 GP Aqua (4.6 × 150 mm, 5 μm) column (Kanto Chemical). The eluent was monitored at 274 nm with a noise-base clean Uni-3 (Union, Gunma, Japan). The mobile phase was 2.5% methanol containing 10 mM sodium acetate (pH 4.5). The flow rate was 1.0 ml/min (0–23 min) and 1.5 ml/min (24–39 min). The column temperature was 35°C. Quantification of the metabolites was performed by comparing the HPLC peak height ratios with that of authentic standards with reference to an internal standard.

Data Analysis. Kinetic parameters were estimated from the fitted curve using a computer program designed for nonlinear regression analysis (KaleidaGraph, Synergy Software, Reading, PA). All the data were analyzed using the mean of duplicated determinations. Data are mean ± S.D. of three independent experiments. Statistical analyses of the kinetic parameters were performed using the two-tailed Student's *t* test. A value of $P < 0.05$ was considered statistically significant.

Results

Coumarin 7-Hydroxylation. To confirm that recombinant CYP2A13 expressed in *E. coli*, which we constructed, is enzymatically active, the coumarin 7-hydroxylase activity was measured. The K_m and V_{max} values by CYP2A13 were 0.7 ± 0.0 μM and 1.7 ± 0.1 pmol/min/pmol P450, respectively. The K_m and V_{max} values in CYP2A6 were 1.3 ± 0.2 μM and 5.0 ± 0.8 pmol/min/pmol P450, respectively. The intrinsic clearance (V_{max}/K_m) of CYP2A13 (2.6 ± 0.1 μl/min/pmol P450) was lower than that of CYP2A6 (3.8 ± 0.7 μl/min/pmol P450).

Ethoxyresorufin *O*-Deethylation and Methoxyresorufin *O*-Demethylation. Using the recombinant CYP2A13, the ethoxyresorufin *O*-deethylase activity and methoxyresorufin *O*-demethylase activity were measured. CYP2A13 exhibited both activities, although the activities were inconsiderable compared with CYP1A1 or CYP1A2. In contrast, CYP2A6 did not show detectable activities. The kinetics by CYP2A13, CYP1A1, and CYP1A2 were fitted to the Michaelis-Menten equation (Fig. 1, A and B). For the ethoxyresorufin *O*-deethylation, the K_m and V_{max} values of CYP2A13 were higher and lower, respectively, than those of CYP1A1 and CYP1A2, resulting in conspicuously lower intrinsic clearance of CYP2A13 than those of CYP1A1 and CYP1A2 (Table 1). Similarly, the intrinsic clearance of CYP2A13 for the methoxyresorufin *O*-demethylation was also lower than those of CYP1A1 and CYP1A2 (Table 1). Thus, CYP2A13 showed slight activities for ethoxyresorufin *O*-deethylation and methoxyresorufin *O*-demethylation.

Phenacetin *O*-Deethylation. We determined whether CYP2A13 catalyzes phenacetin *O*-deethylation, which is known as a typical activity for CYP1A2 (Sesardic et al., 1988). Surprisingly, CYP2A13 showed higher activity for phenacetin *O*-deethylation than CYP1A2 (Fig. 1C). In contrast, CYP2A6 showed scarce activity (0.03 pmol/min/pmol P450) only at a high substrate concentration (250 μM); therefore, the kinetic parameters could not be calculated. The K_m and V_{max} values of CYP2A13 were lower and higher, respectively, than those of CYP1A1 and CYP1A2 (Table 2), resulting in higher intrinsic clearance of CYP2A13 than that of CYP1A2 (2-fold) and CYP1A1 (5-fold).

Theophylline Metabolism. Theophylline is mainly metabolized to three metabolites, 1,3-DMU, 1-MX, and 3-MX by P450s, mainly CYP1A2 in human liver. It has been reported that human lung microsomes can also convert theophylline to 1,3-DMU (Bowen et al., 1991). Because CYP2A13 is highly expressed in the human respiratory tract, we determined whether CYP2A13 is able to metabolize theophylline. As shown in Fig. 1, D and E, CYP2A13 showed metabolic activities for theophylline 8-hydroxylation (1,3-DMU formation) and 3-demethylation (1-MX formation). Interestingly, CYP2A6 also showed activity for theophylline 8-hydroxylation. CYP2A13 showed moderate intrinsic clearance for 8-hydroxylation, following CYP1A2 (Table 3). Although the intrinsic clearance of CYP2A13 was one-tenth that of CYP1A2, it was higher than that of CYP2A6 and CYP1A1. The intrinsic clearance of CYP2A13 for theophylline 3-demethylation was one-sixth that of CYP1A2. Theophylline 1-demethylation (3-MX formation) was detected only by CYP1A2.

Discussion

The *CYP2A13* gene was first cloned in 1995 (Fernandez-Salguero et al., 1995), and the expression of CYP2A13 mRNA in human tissues was determined in 1999 (Koskela et al., 1999). Before 2000, the CYP2A13 protein was assumed to be nonfunctional based on its sequence features of CYP2A13 that resemble the nonfunctional CYP2A7. However, the fact that CYP2A13 is a functional enzyme was first shown by constructing heterologously expressed CYP2A13 in baculovirus-infected insect cells (Su et al., 2000). They reported that CYP2A13 could catalyze coumarin 7-hydroxylation but was much less active than CYP2A6 (0.26 versus 2.2 pmol/min/pmol P450 at 100 μM coumarin concentration). von Weymarn and Murphy (2003) subsequently reported that the K_m and V_{max} values of coumarin 7-hydroxylation by recombinant CYP2A13 in baculovirus-infected insect cells were 0.48 μM and 0.15 pmol/min/pmol P450, respectively. Similarly, He et al. (2004) reported that K_m and V_{max} values by the recombinant CYP2A13 in baculovirus-infected insect cells were 2.2 μM and 0.69 pmol/min/pmol P450, respectively. Thus, the kinetic parameters for coumarin 7-hydroxylation by CYP2A13 obtained in the present study were similar to those of previous results.

Ethoxyresorufin *O*-deethylation, methoxyresorufin *O*-demethylation, and phenacetin *O*-deethylation are used as marker activities for CYP1A2 (Eugster et al., 1993; Tassaneeyakul et al., 1993). Interestingly, the data presented here showed that CYP2A13 could catalyze these reactions. Of particular interest is that CYP2A13 showed higher activity for phenacetin *O*-deethylation than CYP1A2. In contrast to CYP2A13, CYP2A6 hardly catalyzes phenacetin *O*-deethylation. Pre-

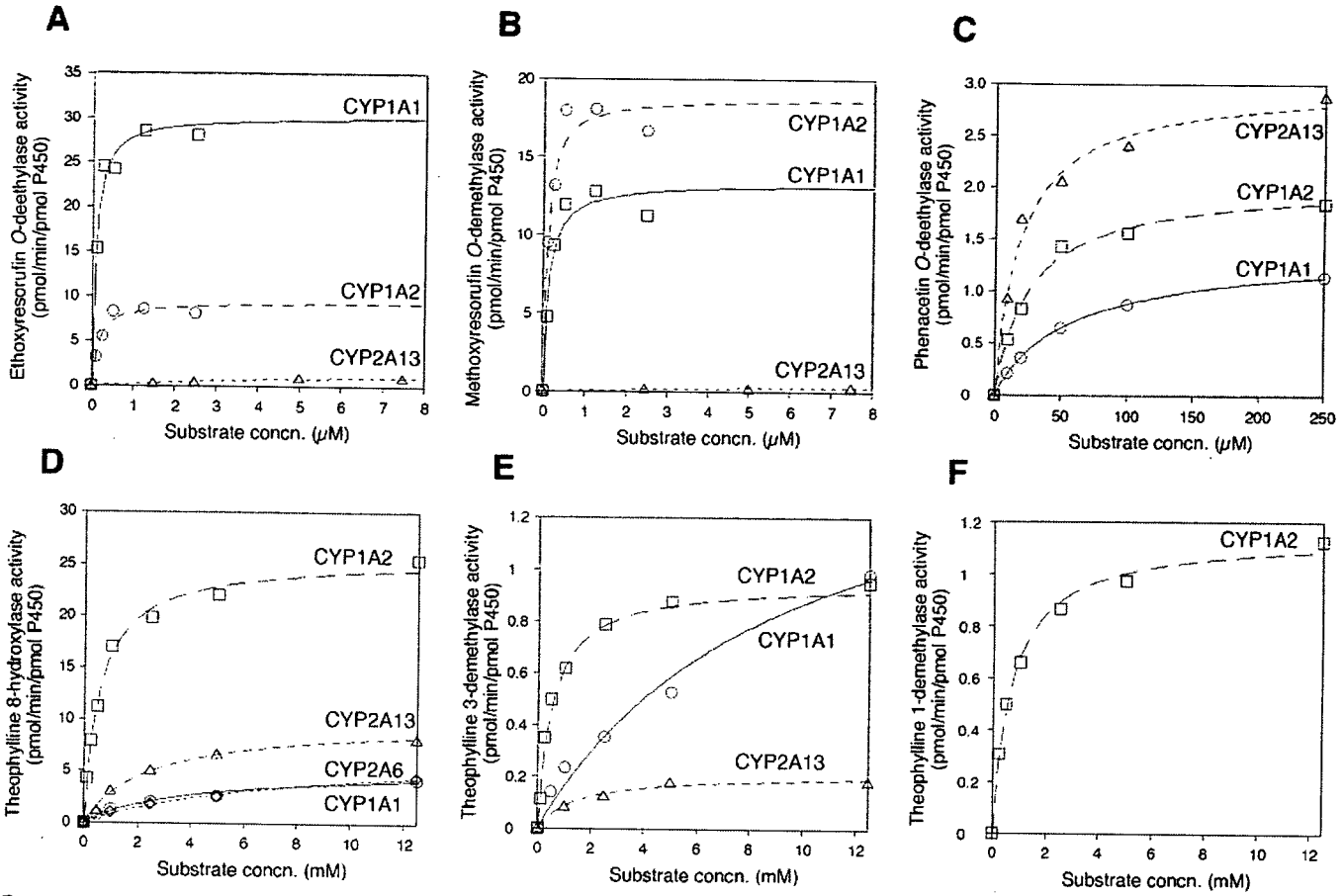

FIG. 1. Kinetic analyses of ethoxyresorufin *O*-deethylation (A), methoxyresorufin *O*-demethylation (B), phenacetin *O*-deethylation (C), theophylline metabolism (D, 8-hydroxylation; E, 3-demethylation; F, 1-demethylation) catalyzed by recombinant CYP1A1, CYP1A2, CYP2A6, and CYP2A13 expressed in *E. coli*. The kinetic parameters were estimated from the fitted curve using the computer program KaleidaGraph designed for nonlinear regression analysis. Each point represents the mean of duplicate determinations.

TABLE 1

Kinetic parameters for ethoxyresorufin O-deethylation and methoxyresorufin O-demethylation by recombinant CYP1As and CYP2As

Data are mean ± S.D. of three independent experiments.

	K_m	V_{max}	V_{max}/K_m
	μM	*pmol/min/pmol P450*	*μl/min/pmol P450*
Ethoxyresorufin *O*-deethylation			
CYP1A1	0.1 ± 0.0	33.5 ± 1.4	321.8 ± 5.2
CYP1A2	0.2 ± 0.0	10.4 ± 1.9	65.7 ± 6.1
CYP2A6	N.D.	N.D.	N.D.
CYP2A13	7.2 ± 1.5[a,b]	2.1 ± 0.3[a,b]	0.3 ± 0.0[a,b]
Methoxyresorufin *O*-demethylation			
CYP1A1	0.1 ± 0.0	13.3 ± 2.1	103.5 ± 11.8
CYP1A2	0.1 ± 0.0	19.9 ± 0.5	177.0 ± 27.5
CYP2A6	N.D.	N.D.	N.D.
CYP2A13	5.9 ± 3.5[a,b]	0.5 ± 0.1[a,b]	0.1 ± 0.0[a,b]

N.D., not detected.
[a] $P < 0.005$ compared with CYP1A1.
[b] $P < 0.005$ compared with CYP1A2.

TABLE 2

Kinetic parameters for phenacetin O-deethylation by recombinant CYP1As and CYP2As

Data are mean ± S.D. of three independent experiments.

	K_m	V_{max}	V_{max}/K_m
	μM	*pmol/min/pmol P450*	*nl/min/pmol P450*
CYP1A1	56.2 ± 2.3	1.5 ± 0.1	26.8 ± 2.7
CYP1A2	29.2 ± 0.4	1.9 ± 0.1	66.4 ± 4.2
CYP2A6	N.A.	N.A.	N.A.
CYP2A13	21.8 ± 2.4[a,b]	2.9 ± 0.3[a,b]	133.2 ± 17.6[a,c]

N.A., not applicable.
[a] $P < 0.005$ compared with CYP1A1.
[b] $P < 0.05$ and [c] $P < 0.005$ compared with CYP1A2.

viously, Venkatakrishnan et al. (1998) reported that the K_m value of CYP2A6 for phenacetin *O*-deethylation was 4098 μM. Thus, phenacetin is a substrate of CYP2A13, but not CYP2A6, even though the amino acid identity between the two enzymes is as high as 93.5%. Rabbit CYP2A isoforms, CYP2A10 and CYP2A11, have been reported to catalyze phenacetin *O*-deethylation (Peng et al., 1993). These isoforms show higher amino acid identity to CYP2A13 rather than CYP2A6, as regards 32 amino acids showing differences between CYP2A6 and CYP2A13 (22 of 32 amino acids correspond to CYP2A13, whereas only 5 of 32 amino acids correspond to CYP2A6). Therefore, these subtle changes in amino acids may contribute to determining the substrate specificity toward phenacetin.

Theophylline is used to manage bronchial asthma and chronic obstructive pulmonary disease. Although it is well known that theophylline is mainly metabolized to 1,3-DMU, 1-MX, and 3-MX by CYP1A2, we first found that CYP2A13 can metabolize theophylline. The clinical significance of CYP2A13 in the metabolism of phenacetin and theophylline in human liver would be limited because systemic clearance of drugs is caused by the metabolism in liver where

TABLE 3

Kinetic parameters for theophylline metabolism by recombinant CYP1As and CYP2As

Data are mean ± S.D. of three independent experiments.

	K_m	V_{max}	V_{max}/K_m
	mM	*pmol/min/pmol P450*	*nl/min/pmol P450*
8-Hydroxylation (1,3-DMU formation)			
CYP1A1	3.9 ± 0.1	5.1 ± 0.2	1.3 ± 0.1
CYP1A2	0.6 ± 0.0	24.4 ± 2.5	40.0 ± 4.0
CYP2A6	8.7 ± 0.4[a,b]	7.4 ± 0.3[a,b]	0.9 ± 0.0[a,b]
CYP2A13	2.5 ± 0.1[a,b]	10.3 ± 0.4[a,b]	4.1 ± 0.2[a,b]
3-Demethylation (1-MX formation)			
CYP1A1	11.1 ± 1.5	1.7 ± 0.2	0.2 ± 0.0
CYP1A2	0.6 ± 0.1	1.0 ± 0.2	1.8 ± 0.3
CYP2A6	N.D.	N.D.	N.D.
CYP2A13	1.4 ± 0.2[a,b]	0.2 ± 0.0[a,b]	0.2 ± 0.0[b]
1-Demethylation (3-MX formation)			
CYP1A1	N.D.	N.D.	N.D.
CYP1A2	0.6 ± 0.1	1.1 ± 0.2	1.8 ± 0.3
CYP2A6	N.D.	N.D.	N.D.
CYP2A13	N.D.	N.D.	N.D.

N.D., not detected.
[a] $P < 0.005$ compared with CYP1A1.
[b] $P < 0.005$ compared with CYP1A2.

CYP2A13 is hardly expressed. However, CYP2A13 is highly expressed in the respiratory tract. It has been shown that human lung is one of the tissues where local metabolism of xenobiotics may take place. Indeed, theophylline is distributed in the lung at the same concentration as in blood (Schack and Waxler, 1949); human lung microsomes can convert theophylline to 1,3-DMU (Bowen et al., 1991). Therefore, CYP2A13 possibly contributes to the theophylline metabolism in human lung and may cause a change in therapeutic efficacy, although other isoforms such as CYP1A1, CYP2E1, CYP2D6, and CYP3A4 expressing in human lung and having capability for theophylline metabolism (Zhang and Kaminsky, 1995; Bernauer et al., 2006) may also contribute to the extrahepatic metabolism.

We found that CYP2A13 shares substrates with CYP1A2. The amino acid homology between CYP2A13 and CYP1A2 is less than 40%. Even if we compared the amino acids within site recognition sites of CYP2A13 and CYP1A2, the amino acid homology is extremely low. In addition, three-dimensional quantitative structure-activity relationship analysis of CYP2A13 is not accomplished yet. Thus, although available information is limited, our data potentially suggested the structural similarity of the substrate binding site of CYP2A13 with that of CYP1A2. Recently, we found that CYP2A13 can catalyze the metabolic activation of 4-aminobiphenyl that is also known to be metabolized by CYP1A2 (Nakajima et al., 2006). Therefore, we investigated whether CYP2A13 is involved in the activation of other arylamines such as 2-aminofluorene, 2-amino-3,5-dimethylimidazo[4,5-*f*]quinoline, and 2-amino-1-methyl-6-phenylimidazo-[4,5-*b*]pyridine that were reported to be activated by CYP1A by umu assay. However, the metabolic activation of these compounds by CYP2A13 was not detected (data not shown). Thus, CYP2A13 may not necessarily be involved in the metabolism of substrates of human CYP1A.

In the present study, we found that CYP2A13 can metabolize several compounds that are known as the substrates of CYP1A2. CYP2A13 may play roles in the local metabolism of drugs in the human respiratory tract. This study significantly increased our understanding of the substrate specificity of human CYP2A13.

Acknowledgments. We thank Brent Bell for reviewing the manuscript.

Drug Metabolism and Toxicology,
Division of Pharmaceutical Sciences,
Graduate School of Medical Science,
Kanazawa University,
Kanazawa, Japan

TATSUKI FUKAMI
MIKI NAKAJIMA
HARUKO SAKAI
MIKI KATOH
TSUYOSHI YOKOI

References

Bao Z, He XY, Ding X, Prabhu S, and Hong JY (2005) Metabolism of nicotine and cotinine by human cytochrome P450 2A13. *Drug Metab Dispos* **33**:258–261.
Bernauer U, Heinrich-Hirsch B, Tonnies M, Peter-Matthias W, and Gundert-Remy U (2006) Characterisation of the xenobiotic-metabolizing cytochrome P450 expression pattern in human lung tissue by immunochemical and activity determination. *Toxicol Lett* **164**:278–288.
Bowen J, Spino M, Tesoro A, Pop R, and Patterson A (1991) Theophylline (theo) biotransformation by human lung microsomes. *Clin Pharmacol Ther* **51**:178.
Bradford MM (1976) Rapid and sensitive method for the quantitation of microgram quantities of protein utilizing the principle of protein-dye binding. *Anal Biochem* **72**:248–254.
Eugster HP, Probst M, Wurgler FE, and Sengstag C (1993) Caffeine, estradiol, and progesterone interact with human CYP1A1 and CYP1A2. Evidence from cDNA-directed expression in *Saccharomyces cerevisiae*. *Drug Metab Dispos* **21**:43–49.
Fernandez-Salguero P, Hoffman SM, Cholerton S, Mohrenweiser H, Raunio H, Rautio A, Pelkonen O, Huang JD, Evans WE, Idle JR, et al. (1995) A genetic polymorphism in coumarin 7-hydroxylation: sequence of the human *CYP2A* genes and identification of variant *CYP2A6* alleles. *Am J Hum Genet* **57**:651–660.
Fukami T, Nakajima M, Yoshida R, Tsuchiya Y, Fujiki Y, Katoh M, McLeod HL, and Yokoi T (2004) A novel polymorphism of human *CYP2A6* gene *CYP2A6*17* has an amino acid substitution (V365M) that decreases enzymatic activity in vitro and in vivo. *Clin Pharmacol Ther* **76**:519–527.
Gallagher EP, Kunze KL, Stapleton PL, and Eaton DL (1996) The kinetics of aflatoxin B_1 oxidation by human cDNA-expressed and human liver microsomal cytochrome P450 1A2 and 3A4. *Toxicol Appl Pharmacol* **141**:595–606.
Gu J, Su Y, Chen QY, Zhang X, and Ding X (2000) Expression and biotransformation enzymes in human fetal olfactory mucosa: potential roles in developmental toxicity. *Toxicol Appl Pharmacol* **165**:158–162.
Hammons GJ, Milton D, Stepps K, Guengerich FP, Tukey RH, and Kadlubar FF (1997) Metabolism of carcinogenic heterocyclic and aromatic amines by recombinant human cytochrome P450 enzymes. *Carcinogenesis* **18**:851–854.
He XY, Shen J, Ding X, Lu AY, and Hong JY (2004) Identification of Val117 and Arg372 as critical amino acid residues for the activity difference between human CYP2A6 and CYP2A13 in coumarin 7-hydroxylation. *Arch Biochem Biophys* **427**:143–153.
He XY, Tang L, Wang SL, Cai QS, Wang JS, and Hong JY (2006) Efficient activation of aflatoxin B_1 by cytochrome P450 2A13, an enzyme predominantly expressed in human respiratory tract. *Int J Cancer* **118**:2665–2671.
Koskela S, Hakkola J, Hukkanen J, Pelkonen O, Sorri M, Saranen A, Anttila S, Fernandez-Salguero P, Gonzalez F, and Raunio H (1999) Expression of *CYP2A* genes in human liver and extrahepatic tissues. *Biochem Pharmacol* **57**:1407–1413.
Nakajima M, Itoh M, Sakai H, Fukami T, Katoh M, Yamazaki H, Kadlubar FF, Imaoka S, Funae Y, and Yokoi T (2006) CYP2A13 expressed in human bladder metabolically activates 4-aminobiphenyl. *Int J Cancer* **119**:2520–2526.
Nakajima M, Kobayashi K, Shimada N, Tokudome S, Yamamoto T, and Kuroiwa Y (1998) Involvement of CYP1A2 in mexiletine metabolism. *Br J Clin Pharmacol* **46**:55–62.
Nakajima M, Yamamoto T, Nunoya K, Yokoi T, Nagashima K, Inoue K, Funae Y, Shimada N, Kamataki T, and Kuroiwa Y (1996) Role of human cytochrome P4502A6 in *C*-oxidation of nicotine. *Drug Metab Dispos* **24**:1212–1217.
Ohyama K, Nakajima M, Suzuki M, Shimada N, Yamazaki H, and Yokoi T (2000) Inhibitory effects of aminodarone and its *N*-deethylated metabolite on human cytochrome P450 activities: prediction of in vivo drug interactions. *Br J Clin Pharmacol* **49**:244–253.
Omura T and Sato R (1964) The carbon monoxide-binding pigment of liver microsomes. *J Biol Chem* **239**:2370–2378.
Parikh A, Gillam EM, and Guengerich FP (1997) Drug metabolism by *Escherichia coli* expressing human cytochromes P450. *Nat Biotechnol* **15**:784–788.
Peng HM, Ding X, and Coon MJ (1993) Isolation and heterologous expression of cloned cDNAs for two rabbit nasal microsomal proteins, CYP2A10 and CYP2A11, that are related to nasal microsomal cytochrome P450 form a. *J Biol Chem* **268**:17253–17260.
Schack JA and Waxler SH (1949) An ultraviolet spectrophotomeric method for the determination of theophylline and theobromine in blood and tissues. *J Pharmacol Exp Ther* **97**:283–291.
Sesardic D, Boobis AR, Edwards RJ, and Davies DS (1988) A form of cytochrome P450 in man, orthologous to form d in the rat, catalyses the *O*-deethylation of phenacetin and is inducible by cigarette smoking. *Br J Clin Pharmacol* **26**:363–372.
Su T, Bao Z, Zhang QY, Smith TJ, Hong JY, and Ding X (2000) Human cytochrome P450 CYP2A13: predominant expression in the respiratory tract and its high efficiency metabolic activation of a tobacco-specific carcinogen, 4-(methylnitrosamino)-1-(3-pyridyl)-1-butanone. *Cancer Res* **60**:5074–5079.
Tassaneeyakul W, Birkett DJ, Veronese ME, McManus ME, Tukey RH, Quattrochi LC, Gelboin HV, and Miners JO (1993) Specificity of substrate and inhibitor probes for human cytochrome P450 1A1 and 1A2. *J Pharmacol Exp Ther* **265**:401–407.
Tiano HF, Hosokawa M, Chulada PC, Smith PB, Wang RL, Gonzalez FJ, Crespi CL, and Langenbach R (1993) Retroviral mediated expression of human cytochrome P450 2A6 in C3H/10T1/2 cells confers transformability by 4-(methylnitrosamino)-1-(3-pyridyl)-1-butanone (NNK). *Carcinogenesis* **14**:1421–1427.
Venkatakrishnan K, von Moltke LL, and Greenblatt DJ (1998) Human cytochromes P450 mediating phenacetin *O*-deethylation in vitro: validation of the high affinity component as an index of CYP1A2 activity. *J Pharm Sci* **87**:1502–1507.